

# Chapter One

## Introduction

Fibroadenoma is the most common lesion of the breast; it occurs in 25% of asymptomatic women (Wakeel, 2003). It is usually a disease of early reproductive life; the peak incidence is between the ages of 15 and 35 years. Conventionally regarded as a benign tumor of the breast, fibroadenoma is also thought to represent a group of hyperplastic breast lobules called “aberrations of normal development and involution (Donegan, 2002).

The lesion is a hormone-dependent neoplasm that lactates during pregnancy and involutes along with the rest of the breast in per menopause (El-Wakeel, 2003). A direct association has been noted between oral contraceptive use before age 20 and the risk of Fibroadenoma (Tavassoli, 1999). The Epstein-Barr virus might play a causative role in the development of this tumor in immunosuppressed patients (Kleer, 2002).

Fibroadenoma presents as a highly mobile, firm, non-tender and often palpable breast mass. Although most frequently unilateral, in 20% of cases, multiple lesions occur in the same breast or bilaterally. Fibroadenoma develops from the special stroma of the lobule. It has been postulated that the tumor might arise from bcl-2-positive mesenchymal cells in the breast, in a manner similar to that proposed for solitary fibrous tumors (Moore, 2001). Macroscopically, the lesion is a well-circumscribed, firm mass, <3 cm in diameter, the cut surface of which appears lobulated and bulging. If the tumor assumes massive proportions (>10 cm), more commonly observed in female adolescents, it is called “giant fibroadenoma.” Microscopically, fibroadenoma consists of a proliferation of epithelial and mesenchymal elements. The stroma proliferates around tubular glands (pericanalicular growth) or compressed cleft-like ducts (intra canalicular growth). Often both types of growth are seen in the same lesion (Tavassoli, 1999).

Ultrasound was discovered as long ago as 1880s. the French Physicist Pierre and their colleague discovered the piezoelectric effect and attempted to develop Piezoelectric materials as senders and receivers of high frequency mechanical disturbance (ultrasound wave) through materials and the industrial use of ultrasound began in 1928s with suggestion of soviet physicist Sokolov, that it could be used to detect flow in materials (Hendee, 2002). The primary of ultrasonic imaging to date has been that of pulse echo mode the principle is very similar to that of sonar In essence, following an ultrasound pulse transmission echoes from median interacted with the object and reflection waves use to build up and construct a picture of the object (Hendee, 2002).

Potential of Ultrasound as an imaging modality was realized as early as the late 1940s, when utilizing sonar and Radar technology during the World War II, finding become practical during the Second World War following the loss of the Titanic. Medical use of ultrasound through the 1930s were confined to therapeutic application such as cancer treatment and physical therapy for various ailments .and several group investigators around the world started exploring diagnostic capabilities of Ultrasound (Goldberg,1989).

In early 1950, John wild and John Ried in Minnesota developed a prototype B-mode ultrasonic imaging instrument and were able to demonstrate the capability of ultrasound for imaging and characterizing a cancerous tissue at frequency as high as 15 MHz And medical diagnostic technology became a widely accepted as diagnostic tool in early 1970s John Wild's pioneering effort and accomplishment were recognized with the Japan Prize In (1991). At the same time apparently unaware of the effort by wild and Reids, Douglas Howry and Joseph of Colorado and Denva also build an ultrasonic imaging device with which they produced across-sectional image of the arm and leg. (Kirk, 2002).

Starting in the late 1940s medical application of ultrasound in Japan were explored by Kenji Tanaka and Toshio wagai were credited with earliest development of ultrasonic Doppler device for monitoring tissue motion and blood flow in 1955. Today ultrasound is the second most utilized diagnostic imaging modality in medicine and is a critically important tool of any medical application. (Kirk, 2002).

Medical ultrasound is a mode of medical imaging that has a wide array of clinical applications, both as a primary modality and as an adjunct to other diagnostic procedures .The basis of its operation is the transmission of high frequency sound into the body followed by the reception, processing, and parametric display of echoes returning from typically a cross-section of the tissue volume under investigation. It is also a soft-tissue modality, given that current, ultrasound methodology does not provide useful images of or through bone or bodies of gas, such as found in the lung and bowel. Its utility in the clinic is in large part due to three characteristics includes It is a real-time modality, does not utilize ionizing radiation and provides quantitative measurement and imaging of blood flow. (Grestner, 1987)

### **1.1. Problem of study:**

Increasing the percentage of using fine needle aspiration for patient suffering from breast fibro adenoma while variable breast test usually may not be sufficient to give the exact diagnosis of Fibroadenoma, Extracting the information not normally detected by human eye .therefore texture analysis technique could reduce or even eliminate the necessity of performing the invasive techniques in addition to ultrasound characteristics might solve the problem and hence save the time , assure quality of diagnosis reduce unnecessary use of fine needle aspiration.

## **1.2. Objective of the study:**

### **1.2.1. General objective:**

The general objective of this study was to characterize breast Fibroadenoma in U/S image by using texture analysis in order to differentiate between the different tissue morphology of breast lesions.

### **1.2.2. Specific Objective:**

- To collate ultrasound finding with age, family history, breast feeding, maternal status.
- To extract texture feature using First order Statistical Textures Texture Analysis (FOS).
- To classify Fibroadenoma and cyst, relative to the normal tissue using Step wise linear discriminate analysis (SW-LDA).
- To establish boundaries between different image region.
- To calculate the sensitivity, specificity and accuracy of each classes

## **1.3. Significant of the Study:**

This study highlighted on classification of breast Fibroadenoma in breast patient using image texture analysis technique and U/S textural pattern in order to actively demonstrate the difference in tissue character depending on the density of the tissue according to the signal measured from ultrasound images where there is no numerical characterisation the diagnosis is based on in U/S

## **1.4. Overview of study:**

This study falls into five chapters classified as: chapter one is an introduction, which include introductory notes on breast Fibroadenoma and texture analysis, as well as statement of the problem and study objectives, in addition to the importance and overview of the study. While

Chapter two includes a comprehensive scholarly literature reviews concerning the previous studies. Chapter three deals with research methodology, where it provides an outline of material and methods used to acquire the data in this study as well as the method of analysis approach. While the results were presented in chapter four, and finally Chapter five include discussion of results, conclusion and recommendation followed by references and appendices.

## **Chapter Two**

### **Literature Review**

#### **2.1. Anatomy and Physiology of Breast:**

The breast is a modified sweat gland that is composed of 15 to 20 lobes that are not well delineated from each other that overlap and that vary greatly in size and distribution. Each lobe consists of parenchymal elements (lobar duct, smaller branch ducts, and lobules) and supporting stromal tissues (compact interlobular stromal fibrous tissue, loose periductal and intralobular stromal fibrous tissue, and fat). The functional unit of the breast is the terminal ductolobular unit (TDLU), which consists of a lobule and its extralobular terminal duct. Each lobule consists of the intralobular segment of the terminal duct, ductules, and loose intralobular stromal fibrous tissue. TDLUs are important because they are the site of origin of most breast pathology and of aberrations of normal development and involution (ANDIs). Most breast carcinomas are thought to arise in the terminal duct near the junction of the intralobular and extralobular segments. Lobar ducts give rise to much less pathology than do TDLUs—mainly large duct and the duct ectasia–periductal mastitis complex. However, most invasive ductal carcinomas papillomas have ductal carcinoma in situ components that can use the ductal system as conduits for growth into other parts of the breast. Each segmental duct has several rows of TDLUs arising from it. Anterior TDLUs tend to have long extralobular terminal ducts, whereas posterior TDLUs tend to have shorter extralobular terminal ducts. Some TDLUs lie at the distal end of the ductal system and are horizontally oriented. Anterior TDLUs are more numerous than posterior and terminal TDLUs, and over time, the posterior TDLUs tend to regress, leaving progressively larger percentage of anterior TDLUs .Because anterior TDLUs greatly outnumber posterior TDLUs,

most breast pathology that arises from TDLUs occurs in the superficial half of the mammary zone, just deep to the anterior mammary fascia. The breast can be divided into three zones, from superficial to deep (Fig. 2-1).

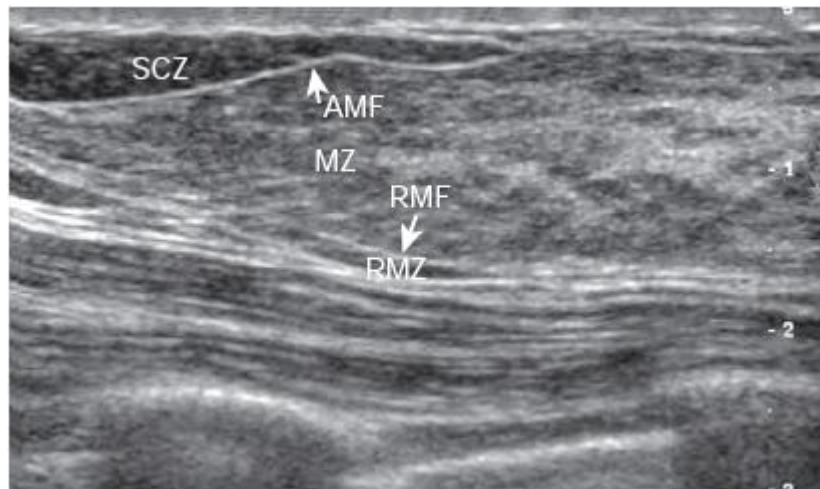


Figure 2-1. Three zones of the breast.

<http://www.ultrasoundpaedia.com/normal-breast>

The most superficial zone is the premammary zone, or subcutaneous zone, which lies between the skin and the anterior mammary fascia. The premammary zone is really part of the integument, and processes that arise primarily within the premammary zone are usually not true breast lesions. Rather, these are lesions of the skin and/or subcutaneous tissues that are identical to those arising from skin and subcutaneous tissues covering any other part of the body (e.g., lipomas, sebaceous cysts). The mammary zone is the middle zone and lies between the anterior mammary fascia and the posterior mammary fascia. It contains the lobar ducts, their branches, most of the TDLUs, and most of the fibrous stromal elements of the breast. The deepest of the zones is the retromammary zone. It mainly contains fat, blood vessels, and lymphatic and is usually much less apparent on sonograms than on mammograms because sonographic

compression flattens the retromammary zone against the chest wall. This differs greatly from mammography, where mammographic compression pulls the retromammary fat away from the chest wall and expands it in the anteroposterior (AP) direction. Because most breast pathology arises from TDLUs and, to a lesser extent, from the mammary ducts, and because most of the ducts and lobules lie within the mammary zone, most true breast pathology arises from the mammary zone. Although lesions that arise within the premammary or retromammary zone are usually skin lesions, true breast lesions that arise within the mammary zone can secondarily involve the premammary and retromammary tissues. (Rumack, 2011).

The mammary fascia that envelops the mammary zone is tough and is relatively more resistant to invasive malignancy than are loose, stromal fibrous tissues. The anterior mammary fascia is continuous with Cooper's ligaments. At the point where it is continuous with alignment, the anterior mammary fascia continues superficially obliquely through the subcutaneous fat, attaches to superficial fascia, and then courses back down through the subcutaneous fat, where it continues on as anterior mammary fascia. Each Cooper's ligament is composed of two closely applied layers of anterior mammary fascia with a potential space inferiorly, where the two layers separate and course away from each other as anterior mammary fasciae (Fig. 2-2).



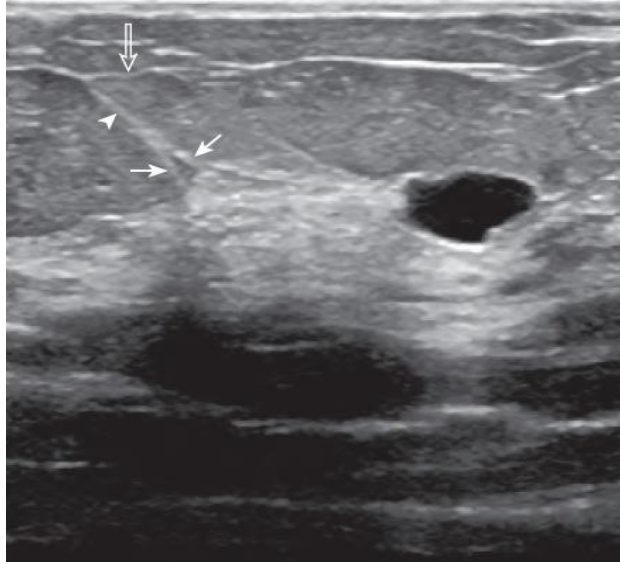


Figure 2-2. Mammary fasciae and Cooper's ligaments.

<http://www.ncbi.nlm.nih.gov/pmc/articles/PMC2766883/figure/F0001/>

This affects the sonographic appearance of invasive malignancies, as discussed later. The normal anatomic structures of the breast span a spectrum of echogenicities, from midlevel gray to intensely hyperechoic. Hyperechoic normal structures include compact interlobular stromal fibrous tissue, anterior and posterior mammary fasciae, Cooper's ligaments, and skin. Duct walls, when visible, also appear hyperechoic. Normal structures that have midlevel echogenicity (isoechoic) include fat, epithelial tissues in ducts and lobules, and loose, intralobular and periductal, stromal fibrous tissue. Water density tissue on mammography corresponds to a variety of different normal tissues that can be shown sonographically. Dense interlobular stromal fibrous tissue, loose periductal or intralobular stromal fibrous tissue, and epithelial elements in duct and lobules all appear to be of equal density mammographically.

Mammographically dense tissue can correspond to purely hyperechoic, purely isoechoic, or mixed hyperechoic and isoechoic tissues on sonography (Fig. 2-3).

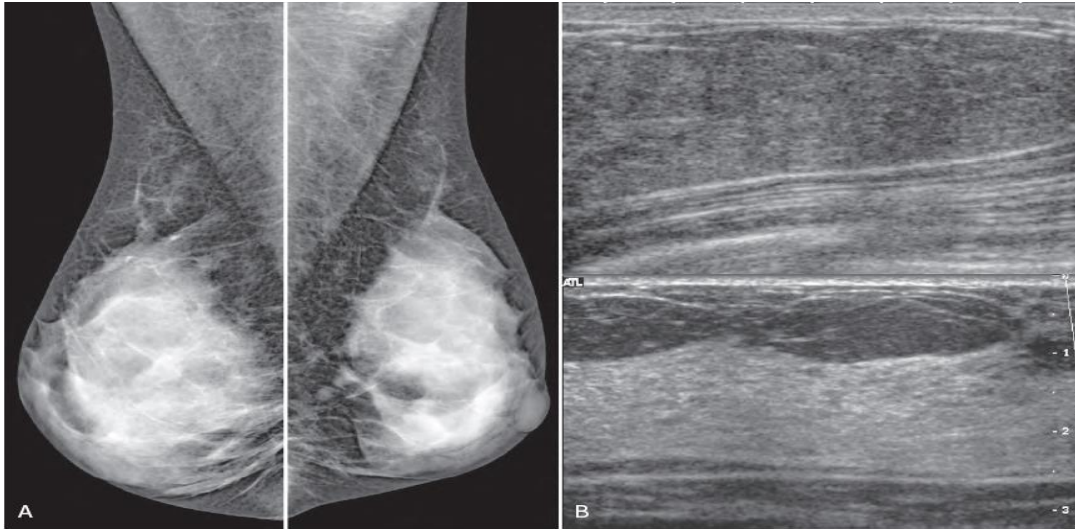
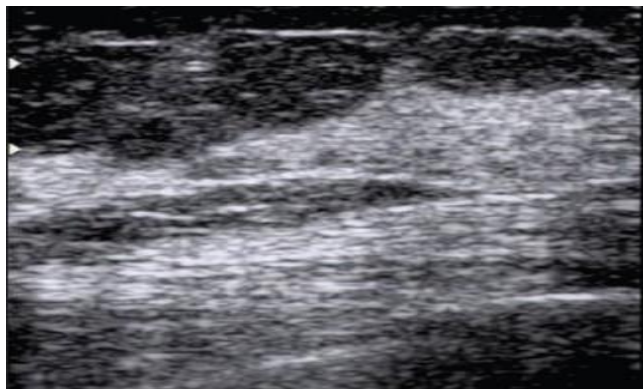


Figure 2-3. Dense breast tissue: radiographic-sonographic correlation. Radiographically dense (water density) tissue on mammograms (A) can correspond to two different types of tissue on sonography: B, almost-isochoric glandular tissue, and C, intensely hyperechoic interlobular stromal fibrous tissue.

<http://www.diagnosticimaging.com/ultrasound/image-iq-ultrasound-screening-dense-breasts>

Most contain mixtures of fibrous and glandular elements interspersed with variable amounts of fat (Fig. 2-4 ). Over time, atrophy tends to occur more rapidly in the areas of the mammary zone that lie between Cooper's ligaments, leaving progressively more of the residual fibroglandular elements within these ligaments



(Fig. 2-4) Echogenic breast parenchyma surrounded by hypoechoic fat

<http://www.ncbi.nlm.nih.gov/pmc/articles/PMC2766883/figure/F0001/>

Normal mammary ducts that are not ectatic can appear in two ways sonographically. A mammary duct can appear purely isoechoic when the centrally located hyperechoic duct wall cannot be visualized because of poor angle of incidence or suboptimal transducer resolution—when only the loose periductal stromal fibrous tissue is visible. A mammary duct can also be shown as a central, bright echo surrounded by isoechoic loose stromal fibrous tissue when the apposed walls of the central duct can be optimally demonstrated. It is common for a single duct to have both sonographic appearances, depending on the angle of incidence with the duct walls. Variable degrees of ductal ectasia become increasingly common with age, particularly within the lactiferous sinus portion of the lobar duct in the subareolar region. In ectatic ducts, anechoic or hypoechoic fluid separates the two duct walls and compresses the loose periductal stromal tissues to variable degrees (Fig. 2-5, A and B). Duct ectasia occurs in up to 50% of women over age 50 and usually is asymptomatic. In certain patients, however, ductal ectasia may be associated with nipple discharge or may lead to periductal mastitis and its acute and chronic complications. (Rumack, 2011).

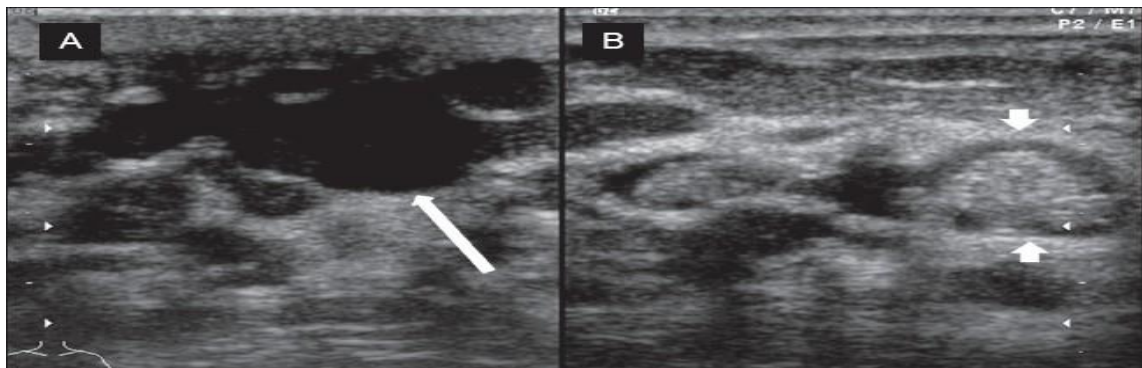


Figure 2-5 (A& B) Chronic duct ectasia. Longitudinal image (A) shows a dilated duct containing inspissated debris (arrow) is seen. In cross section (B), the intraductal debris may appear as a focal lesion (arrowheads)

<http://www.ncbi.nlm.nih.gov/pmc/articles/PMC2766883/figure/F0004>

The ducts within the nipple and immediate subareolar regions are poorly seen when scanned from straight anteriorly because they course almost parallel to the beam in those locations. However, special maneuvers designed to improve the angle of incidence enable adequate demonstration of the entire mammary duct through out the subareolar region, even within the nipple when necessary. These maneuvers include the peripheral compression technique, two-handed compression technique, and rolled nipple technique. These maneuvers are most useful when evaluating patients with nipple discharge and in assessing malignant nodules for extensive intraductal involvement growing within the duct toward the nipple. The two-handed compression technique is also useful in assessing gynecomastia. Individual TDLUs may be sonographically visible—under ideal conditions—as small isoechoic structures. Normal TDLUs are about 2 mm in diameter but may be as large as 5 mm in patients with fibrocystic change, adenosis, or other ANDIs (Fig. 2-6). In patient's who are pregnant or lactating and in patients with adenosis, not only are TDLUs enlarged, but they are also increased in number. In certain cases, TDLUs become large and numerous enough to form continuous sheets of isoechoic tissue. The variable prominence of TDLUs creates a continuous spectrum in the appearance of breast tissue from TDLUs that are not visible to breasts that appear to be totally isoechoic (Fig. 2-6). This most often occurs anteriorly, where lobules are most numerous, but in certain cases can fill and distend the entire mammary zone. One of the most valuable features of high-frequency coded

harmonic imaging is that it tends to make pathologic solid nodules appear relatively more hypoechoic and conspicuous in a background of isoechoic tissues, reducing the chance that such a nodule will not be detected and distinguished from normal lobules. (Rumack, 2011).

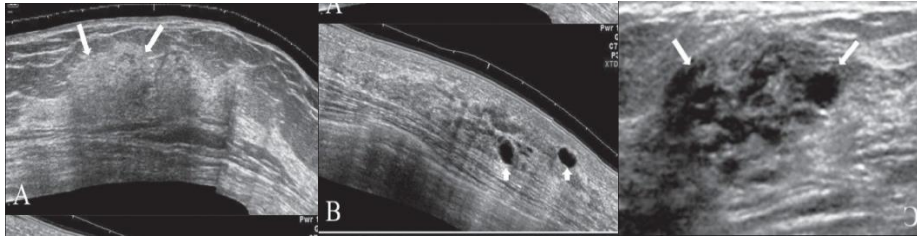


Figure 2-6: A, B, C Fibrocystic change. Extended view images (A, B) show a focal area of thickening of the breast parenchyma (A) with patchy increase in echogenicity (arrows) and scattered, discrete, thin-walled cysts (arrowheads in B).

<http://www.ncbi.nlm.nih.gov/pmc/articles/PMC2766883/figure/F0003/>

Lymphatic drainage from most of the breast is from deep to superficial, toward the sub dermal lymphatic network, then to the periareolar plexus (Sappey's plexus), and finally on to the axilla. Some of the deep portions of the breast, particularly medially, preferentially drain along the chest wall to the internal mammary lymph nodes. Most drainage of the breast is to the axillary lymph nodes. Most lymphatic metastases from the breast are to the axilla, with a minority occurring in the internal mammary lymph nodes. The three levels of axillary lymph nodes are determined by their location relative to the pectoralis minor muscle. Lymph nodes that lie peripheral to the inferolateral edge of the pectoralis minor are level 1 lymph nodes; nodes that lie posterior to the pectoralis minor muscle are level 2 lymph nodes; and nodes that lie proximal to the super medial border of the pectoralis minor muscle are level 3 lymph nodes or infraclavicular nodes. Lymphatic drainage to the axilla usually passes through level 1, then level 2, and finally to level 3 lymph nodes (Fig. 2- 7).

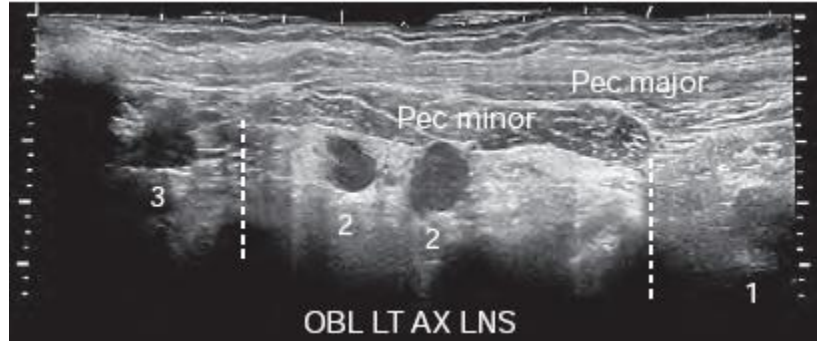


Figure 2-7 Pectoralis minor muscle and levels of axillary lymph nodes.

<http://www.ncbi.nlm.nih.gov/pmc/articles/PMC2766883/figure/F0002/>

From level 3 nodes, metastases may progress to internal jugular or supra clavicular lymph nodes. Rotter nodes lie between the pectoralis major and pectoralis minor muscles. It is important to recognize level 2 and 3 lymph nodes and Rotter lymph node metastases, because unrecognized and untreated metastases to these lymph nodes are a frequent source of so-called chest wall recurrences. (Rumack, 2011).

Internal mammary nodes lie in a chain parallel to the internal mammary artery and veins along the deep side of the chest wall, just lateral to the edges of the sternum. Metastases most often involve internal mammary lymph nodes in the second and third interspaces. Using color Doppler sonography to identify the internal mammary vessels can be helpful in finding abnormal internal mammary lymph nodes. Normal internal mammary lymph nodes can be identified under ideal circumstances, but not in all patients. (Rumack, 2011).

A significant percentage of patients have lymph nodes that lie within the breast, intramammary lymph nodes. These can lie anywhere within the breast but are most common in the axillary segment just below the axilla. They usually lie within a centimeter of the posterior mammary artery, a branch of the axillary artery that extends from the axilla toward the nipple.

Intramammary lymph nodes can also be found occasionally in the medial edge of the breast superficial to the internal mammary lymph nodes. These medial lymph nodes are seen much less frequently on mammography than on sonography because mammographic compression can seldom pull them far enough away from the chest wall to be mammographically visible. Medial intramammary lymph nodes can be difficult to demonstrate sonographically without the use of an acoustic stand off because of their superficial location just beneath the skin. Breast cancer metastases can involve the supra clavicular lymph nodes, but these nodes are positive only when lymph node metastases are extensive. Metastases must involve levels 1, 2, and 3 axillary lymph nodes or internal mammary and internal jugular lymph nodes before reaching the supra clavicular nodes. The first lymph node to which lymphatic drainage flows and the first node involved by metastases has been termed the sentinel lymph node. The location of the sentinel node varies, depending on the location of the primary tumor within the breast. The sentinel lymph node is usually a level 1 axillary lymph node, but in certain cases, it may be an intramammary node or even a level 2 node. Occasionally, the sentinel node may be an internal mammary node. (Rumack, 2011).

## **2.2. Benign Breast Disease:**

The vast majority of the lesions that occur in the breast are benign. Much concern is given to malignant lesions of the breast because breast cancer is the most common malignancy in women in western countries; however, benign lesions of the breast are far more frequent than malignant ones. With the use of mammography, ultrasound, and magnetic resonance imaging of the breast and the extensive use of needle biopsies, the diagnosis of a benign breast disease can be accomplished without surgery in the majority of patients. Because the majority of benign lesions

are not associated with an increased risk for subsequent breast cancer, unnecessary surgical procedures should be avoided. (Caleffi, 2001).

The term “benign breast diseases” encompasses a heterogeneous group of lesions that may present a wide range of symptoms or may be detected as incidental microscopic findings. The incidence of benign breast lesions begins to rise during the second decade of life and peaks in the fourth and fifth decades, as opposed to malignant diseases, for which the incidence continues to increase after menopause, although at a less rapid pace. In this review, the most frequently seen benign lesions of the breast are summarized as developmental abnormalities, inflammatory lesions, fibrocystic changes, stromal lesions, and neoplasm’s (Vecchia, 1985).

**Fibrocystic Changes:** Fibrocystic changes (FCCs) constitute the most frequent benign disorder of the breast. Such changes generally affect premenopausal women between 20 and 50 years of age (Vecchia, 1985). Although many other names have been used to describe this entity over the years, (including fibrocystic disease, cystic mastopathy, chronic cystic disease, mazoplasia, Reclus’s disease), the term “fibrocystic changes” is now preferred, because this process is observed clinically in up to 50% and histologically in 90% of women (Kinoshita, 2002). FCCs may be multifocal and bilateral. The most common presenting symptoms are breast pain and tender nodularities in breasts. Although the exact pathogenesis of the entity is not clear, hormonal imbalance, particularly estrogen predominance over progesterone, seems to play an important role in its development. (Vorherr, 1986). FCCs comprise both cysts (macro and micro) and solid lesions, including adenosis, epithelial hyperplasia with or without a typia, a porcine metaplasia, radial scar, and papilloma. Over the years, it has been one of the major issues to determine whether these lesions are a risk factor for the subsequent development of breast cancer. As the use of mammography and the identification of benign breast diseases become



more common, it is crucial to identify women who are at an increased risk for breast cancer. (Vorherr, 1986).

**Cysts:** Is fluid-filled, round or ovoid structures that are found in as many as one third of women between 35 and 50 years old. Although most are subclinical “micro cysts,” in about 20%–25% of cases, palpable (gross) cystic change, which generally presents as a simple cyst, is encountered. Cysts cannot reliably be distinguished from solid masses by clinical breast examination or mammography; in these cases, ultrasonography and fine needle aspiration (FNA) cytology, which are highly accurate, are used. (Houssami, 2005).

Cysts are derived from the terminal duct lobular unit. In most cysts, the epithelial lining is either flattened or totally absent. In only a small number of cysts, a porcine epithelial lining is observed. Because gross cysts are not associated with an increased risk of carcinoma development, the current consensus on the management of gross cysts is routine follow-up of the patient, without further therapy. (Houssami, 2005). Complex (or complicated or atypical) cyst is a sonographic diagnosis that is characterized by internal echoes or thin septations, thickened and/or irregular wall, and absent posterior enhancement. (Venta, 1999). They are reported in approximately 5%–5.5% of all breast ultrasound examinations. The malignancy rate of complex cysts, which is 0.3% as described by Venta, is lower than that for lesions classified as “probably benign.” These patients can be managed with follow-up imaging studies ;( Venta, 1999). However, if the lesion also includes an intracystic mass (intracystic nodule), it should be regarded as “suspicious for neoplasm” and managed as solid lesions. Either a core needle biopsy or surgical biopsy is indicated for these lesions (Venta, 1999).

**Adenosis the breast** is a proliferative lesion that is characterized by an increased number or size of glandular components, mostly involving the lobular units. Various types of adenosis have

been described, of which sclerosing adenosis and micro glandular adenosis merit detailed description (Jensen, 1989).

Sclerosing adenosis of the breast is defined as a benign lobulocentric lesion of disordered acinar, my epithelial, and connective tissue elements, which can mimic infiltrating carcinoma both grossly and microscopically (Gill, 2003). Sclerosing adenosis can manifest as a palpable mass or as a suspicious finding at mammography. It is strongly associated with various proliferative lesions, including epithelial hyperplasia, intraductal or sclerosing papilloma, complex sclerosing lesion, calcification, and a pocrine changes. It can coexist with both invasive and in situ cancers (Millis, 1995).

Micro glandular adenosis of the breast is characterized by a proliferation of round, small glands distributed irregularly within dense fibrous and/or adipose tissue. Most of the glandular structures have open Lumina in which eosinophilic material is usually seen. The most important histological feature of micro glandular adenosis is that it may lack the outer myoepithelial layer seen in other types of adenosis. The lack of myoepithelial layer makes it harder to differentiate micro glandular adenosis from tubular carcinoma (Eusebi, 1995). However, the presence of basal lamina encircling glandular structures, which can also be shown by lamin in or type IV collagen immunohistochemical stains, and the absence of epithelial membrane antigen staining in the luminal epithelial cells distinguish micro glandular adenosis from tubular carcinoma (Acs,2003). Although micro glandular adenosis is considered benign, there is some evidence of the potential of this lesion to become invasive carcinoma. Micro glandular adenosis also has a tendency to recur if not completely excised (Tavassoli, 1999).

**Metaplasia:** Apocrine metaplasia is characterized by the presence of columnar cells with abundant granular, eosinophilic cytoplasm and luminal cytoplasmic projections or apical snouts.

These cells line dilated ducts or can be seen in papillary proliferations. They are more frequently found in younger women. All normal and metaplastic apocrine cells can be stained with gross cystic disease fluid protein 15. Clear cell metaplasia of the breast is a rare lesion. Its significance comes from its morphologic similarity to clear cell carcinoma. However, the similarity of its immunohistochemical staining profile with that of eccrine sweat glands suggests that clear cell metaplasia may in fact represent “eccrine metaplasia” (Tavassoli, 1999).

**Epithelial Hyperplasia** :( ductal or lobular type) is one of the most challenging FCCs to diagnose properly. Epithelial hyperplasia is the most common form of proliferative breast disease. It can be difficult to distinguish between ductal and lobular hyperplasia. In addition, it can also be difficult to distinguish between usual ductal or lobular hyperplasia and their atypical counterparts—“atypical ductal hyperplasia and atypical lobular hyperplasia” (Tavassoli, 1999).

**Ductal Lesions:** Normally, breast ducts are lined by two layers of low cubical cells with specialized luminal borders and basal contractile myoepithelial cells. Any increase in cell number within the ductal space is regarded as epithelial hyperplasia. Further classification is based on the degree and architectural and cytologic features of the proliferating cells. Usual ductal hyperplasia or simple hyperplasia denotes an increased number of cells without architectural distortion or distention of the ductal contour. Usual ductal hyperplasia does not increase the risk for breast cancer. In mild hyperplasia of the usual type, proliferating epithelial cells are a three- to four-cell layer, whereas moderate hyperplasia describes epithelial proliferation more than four cells thick, often with accompanying bridging of the luminal space. In florid hyperplasia, the lumen is distended and may be obliterated. The most important cytologic features of mild, moderate, or florid epithelial hyperplasia are an admixture of cell types (epithelial cells, myoepithelial cells, and metaplastic apocrine cells) and variation in the

appearances of epithelial cells and their nuclei (Koerner, 2004). The term atypical ductal hyperplasia is defined as a type of a ductal hyperplasia that morphologically mimics low-grade ductal carcinoma in situ (DCIS). Characteristically, it has a uniform population of cells. Most lesions of atypical ductal hyperplasia are small and focal. They involve only a portion of a duct or only a few small ducts measuring <2 mm. (Koerner, 2004). With the increasing use of mammography, and detection of calcifications, hyperplasia is being diagnosed more frequently. Women with atypical ductal hyperplasia develop cancer usually within 10–15 years of the diagnosis. The risk for cancer declines after 15 years .The risk for breast cancer in women with atypical ductal hyperplasia is also related to the patient’s menopausal status (Koerner, 2004).

**Lobular Lesions:** Lobular-type epithelial proliferations, both atypical lobular hyperplasia and lobular carcinoma in situ, are collectively termed lobular neoplasia because, unlike ductal lesions, which exhibit heterogeneous morphologic features, the histologic features of lobular type epithelial proliferations are very similar, and the only difference between atypical lobular hyperplasia and lobular carcinoma in situ is the extent and degree of epithelial proliferation. Because both lesions are regarded and managed as a risk factor rather than well-established precursor lesions, lobular neoplasia terminology has gained general acceptance. Lobular neoplasia is a relatively rare breast lesion. It rarely manifests itself clinically. Lobular neoplasia is identified as an incidental finding in biopsies excised for other abnormalities. The frequency of detection depends on the volume of tissue removed during surgery and extent of histological examination. Lobular neoplasia is most prevalent in premenopausal women. It is a multifocal lesion, and many patients have lesions involving multiple quadrants of the breast. Both atypical lobular hyperplasia and lobular carcinoma in situ increase the risk for the subsequent development of invasive carcinoma, by about fourfold for atypical lobular hyperplasia and

tenfold for lobular carcinoma in situ. Although subsequent carcinomas can occur in either breast without a direct relationship to the previous site of biopsy, in a recent retrospective study.(Page, 2002) reported that the development of invasive carcinoma after atypical lobular hyperplasia was three times more likely to arise in the ipsilateral breast than in the opposite breast. Invasive carcinomas may arise 15–20 years after diagnosis. Systemic follow-up and appropriate risk assessment is recommended for patients with lobular neoplasia. (Schnitt, 2003).

**Columnar Cell Lesions:** Represent a spectrum of lesions that have been encountered with increasing frequency in needle core breast biopsies because these lesions are commonly associated with micro calcifications and detected by mammographic screening. A working classification of these lesions has been proposed by Schnitt and Vincent-Salomon (Schnitt, 2003). As columnar cell change and columnar cell hyperplasia, each of which may have a *typia* or not. Ongoing studies on the clinical significance of atypical columnar cell lesions, which are also known as flat epithelial *typia*, have shown that the likelihood of local recurrence or progression to invasive breast cancer is exceedingly low. However, based on the foregoing observations, it has been suggested that at least some lesions are probably neoplastic proliferations that may represent either a precursor of low-grade DCIS or even invasive carcinoma, particularly tubular carcinoma. (Schnitt, 2003).

**Fibroadenoma:** is the most common lesion of the breast; it occurs in 25% of asymptomatic women. It is usually a disease of early reproductive life; the peak incidence is between the ages of 15 and 35 years. Conventionally regarded as a benign tumor of the breast, fibroadenoma is also thought to represent a group of hyperplastic breast lobules called “aberrations of normal development and involution”. (Hughes, 1989). The lesion is a hormone-dependent neoplasm that lactates during pregnancy and involutes along with the rest of the breast in per menopause.

(Tavassoli, 1999). A direct association has been noted between oral contraceptive use before age 20 and the risk of Fibroadenoma. (Kleer, 2002). The Epstein-Barr virus might play a causative role in the development of this tumor in immunosuppressed patients (Moore, 2001).

Fibroadenoma presents as a highly mobile, firm, non-tender and often palpable breast mass. Although most frequently unilateral, in 20% of cases, multiple lesions occur in the same breast or bilaterally. Fibroadenoma develops from the special stroma of the lobule. It has been postulated that the tumor might arise from bcl-2-positive mesenchymal cells in the breast, in a manner similar to that proposed for solitary fibrous tumors (Franco, 2003). Macroscopically, the lesion is a well-circumscribed, firm mass, <3 cm in diameter, the cut surface of which appears lobulated and bulging. If the tumor assumes massive proportions (>10 cm), more commonly observed in female adolescents, it is called “giant fibroadenoma.” Microscopically, fibroadenoma consists of a proliferation of epithelial and mesenchymal elements. The stroma proliferates around tubular glands (pericanalicular growth) or compressed cleft-like ducts (intra canalicular growth). Often both types of growth are seen in the same lesion. (Kler, 2002).

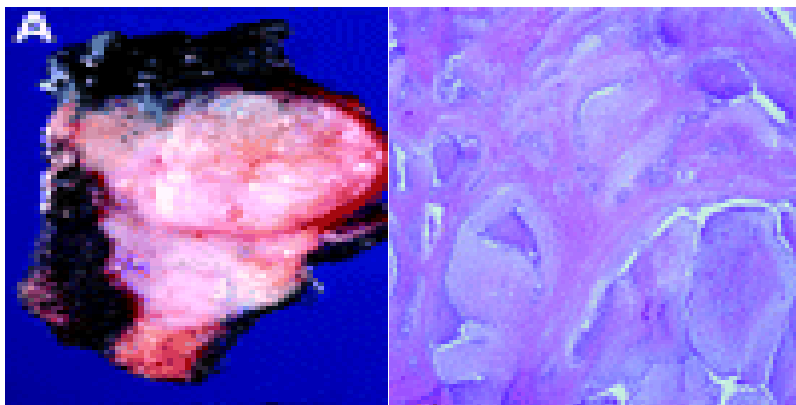


Figure: 2-8 Fibroadenoma. (A): The cut surface of fibroadenoma is lobulated, solid, and gray-white, with a characteristic bulging appearance. (B): Histologically the lesion consists of densely fibrotic stroma and compressed cleft-like ducts.

<http://theoncologist.alphamedpress.org/content/11/5/435/F4.expansion.html>

Cytogenetic studies have reported chromosomal aberrations in both epithelial and stromal cells, suggesting that the two components may involve neoplastic changes (Valdes a, 2005). Phyllodes tumor is a fibroepithelial tumor of the breast with a spectrum of changes. Benign phyllodes tumor is usually difficult to differentiate from fibroadenoma. Hyper cellular stroma with cytologic atypia, increased mitoses, and infiltrative margins of the lesion are the most reliable discriminators to separate lesions with recurrence and malignant behavior. In terms of surgical treatment of these tumors, it is important to recognize phyllodes tumor because it should be excised completely with clear margins to obviate any chance of local recurrence. In cases of recurrent disease, mastectomy is often performed. (Chen, 2005).

Approximately 50% of fibroadenomas contain other proliferative changes of breast, such as sclerosing adenosis, adenosis, and duct epithelial hyperplasia. Fibroadenomas that contain these elements are called complex fibroadenomas. Simple fibroadenomas are not associated with any increased risk for subsequent breast cancer. However, women with complex fibroadenomas may have a slightly higher risk for subsequent cancer. The presence of atypia (either ductal or lobular) confined to a fibroadenoma does not lead to a greater risk for long-term breast carcinoma compared with fibroadenomas in general. (Shabtai,2001).

Fibroadenomas in older women or in women with a family history of breast cancer have a higher incidence of associated carcinoma. (Hughes,1989) show that the relative risk of developing breast cancer in patients who had surgically excised fibroadenomas increases in the presence of complex features within the fibroadenomas, ductal hyperplasia, or a family history of breast carcinoma (in a first-degree relative). Progressive somatic genetic alterations that are associated with the development of breast cancer have been studied in fibroadenomas. No genetic instabilities, manifested as loss of heterozygosity or microsatellite instability, have been found in

any fibroadenoma components regardless of their association with breast cancer or their histologic complexity. (Boolbol, 2005).

The current management of patients with clinically or radiologically suspected fibroadenoma varies. Some physicians prefer excision for tissue diagnosis, but conservative management will likely replace surgical treatment in the near future, on the basis of the young age of the patient, findings of benign imaging and clinical characteristics, and benign findings on either FNA biopsy or needle core biopsy (Shabtai, 2001). Minimally invasive techniques, such as ultrasound-guided cryoablation, seem to be an excellent treatment option for Fibroadenoma in women who wish to avoid surgery. (Caleffi, 2004) or else the lesion may simply be treated with observation and followed up periodically. Juvenile Fibroadenoma is a variant of Fibroadenoma that presents between 10 and 18 years of age, usually as a painless, solitary, unilateral mass >5 cm. It can reach up to 15 or 20 cm in dimension, so although it is an entirely benign lesion, surgical removal is recommended. (Lanng,2004)

## **2.3. Breast imaging:**

### **2.3.1. Breast Mammography:**

Also called mastography, is the process of using low-energy X-rays (usually around 30 KVp) to examine the human breast, which is used as a diagnostic and screening tool. The goal of mammography is the early detection of breast cancer, typically through detection of characteristic masses and/or micro calcifications like all X-rays, mammograms use doses of ionizing radiation to create images. These images are then analyzed for any abnormal findings. It is normal to use lower-energy X-rays, typically Mo (K-shell x-ray energies of 17.5 and 19.6 keV) and Rh (20.2 and 22.7 keV) than those used for radiography of bone Ultrasound ductography, positron emission mammography (PEM), and magnetic resonance imaging (MRI)



are adjuncts to mammography. Ultrasound is typically used for further evaluation of masses found on mammography or palpable masses not seen on mammograms. Instance from breast-conserving lumpectomy to other procedures being investigated include tomosynthesis. (Basset and Kimme, 1991).

The American College of Radiology and American Cancer Society recommend yearly screening mammography starting at age 40. The Canadian Task Force on Preventive Health Care (2012) and the European Cancer Observatory (2011) recommends mammography every 2–3 years between 50 and 69.( Egan, 1988) these task force reports point out that in addition to unnecessary surgery and anxiety, the risks of more frequent mammograms include a small but significant increase in breast cancer induced by radiation.(Kopans,1984). Additionally, mammograms should not be done with any increased frequency in people under going breast surgery, including breast enlargement, mastopexy, and breast reduction. (Kopans, 1984) the authors conclude that the time has come to re-assess whether universal mammography screening should be recommended for any age group. (Tohno, 1994) they thus state that universal screening may not be reasonable. Mammography has a false-negative (missed cancer) rate of at least 10 percent. This is partly due to dense tissues obscuring the cancer and the fact that the appearance of cancer on mammograms has a large overlap with the appearance of normal tissues. A meta-analysis review of programs in countries with organized screening found 52% over-diagnosis. (Wilson, (1997)

### **2.3.2. Magnetic Resonance Imaging:**

Early studies using magnetic resonance imaging (MRI) for breast imaging were performed without contrast agents (unenhanced MRI). However, unenhanced MRI with various combinations of pulse sequences has not proved helpful for detection or diagnosis of breast

cancer. The use of contrast agents, as initiated by Heywang in 1986 and 1988, is now considered mandatory for detection and diagnosis of breast cancer by MRI. Contrast enhanced. Breast MRI today implies that both breasts are imaged with high spatial resolution before and at least two or three times after intravenous administration of a standard MR contrast agent (so-called “dynamic contrast-enhanced breast MRI”). Both morphology of a lesion (before and after contrast administration) and its enhancement dynamics contribute to the diagnostic information that may be provided only by MRI. Unenhanced MRI using specific sequences has proven useful for detection or exclusion of implant failure. (Heywang, 1997).

Overall, MRI has proved to be the most sensitive method for the detection of invasive breast cancer, with reported sensitivities for invasive breast cancer ranging around 85–97%. The sensitivity for DCIS is lower, and in this context MRI is complementary to mammography. The specificity of MRI is lower than that of mammography. It is essential that MR-guided interventions must be available to further assess lesions that are detected and visible only by MRI. Even though the accuracy of MRI is not sufficient to replace biopsy, in experienced hands the addition of MRI may in some instances allow improvement of sensitivity and/or specificity and better select patients who require biopsy. (Heywang, 1997).

Contrast-enhanced MRI is not indicated as a screening method for young patients with dense or lumpy breast tissue. The reasons are as follows: MRI has a high sensitivity for detection of occult benign changes (e.g., fibroadenomas, areas of adenosis) in at least 15% of patients. Areas of transient enhancement due to hormonal influences, which may be another cause of false positive calls, may be more frequent in this age group. And at the same time, the prevalence of malignancy is by far lower than that of benign disease. Therefore, contrast-enhanced MRI might

necessitate an unacceptably high number of workups for benign changes in young patients without high genetic risk, while detecting very few, if any, malignancies. (Lowry, 2012)

Finally, MRI is generally not necessary for evaluation of palpable, mammographically or sonographically visible masses, since percutaneous biopsy owing to its lower false positive rate is much more cost-effective. Contrast-enhanced MRI for early detection of malignancy is, however, indicated for screening of young women at high-risk, who (after diligent counseling) for imaging surveillance. (Considering that both mammography and MRI may offer complementary information) .while neither method alone has 100% sensitivity, alternating screening using MRI and mammography every 6 months may be the most effective alternative (Lowry,2012).

### **2.3.3. Scintimammography:**

It is an examination that use Radiopharmaceutical  $^{99m}\text{Tc}$ -sestamibi (hexakis [2 methoxyisobutylisonitril]),  $^{99m}\text{Tc}$ -tetrofosmin (1, 2-bis[2-ethoxyethyl] phosphino) ethane to detect and localize breast carcinoma, particularly in women with palpable breast . Usually done in conjunction with and to help improve the sensitivity and specificity of mammography, and aid in decisions about biopsy. Evaluation of women with mammographically dense breasts, palpable mass, and negative fine needle aspiration (FNA).Detection and localization of metastases in the axillary lymph nodes. Test helps breast cancer patients decide between lumpectomy and mastectomy, for high-risk patients with prior history or family history of premenopausal breast cancer, patients with palpable lumps or abnormal lesions on mammography, and patients with dense, as opposed to fatty, breast tissue. Evaluation of known but non palpable breast lesions , elevated tumor markers ,therapy ,breast implants, abnormal findings on other related diagnostic images, e.g., PET, MRI, CT, US, mammography.

Differentiation between true-positives (e.g., invasive ductal carcinoma, ductal carcinoma in situ, colloid carcinoma, medullary carcinoma, and infiltrating lobular carcinoma) and true negatives (e.g., fibrocystic changes, fibroadenoma, atypical ductal hyperplasia, florid epithelial hyperplasia, stromal sclerosis, complex sclerosing lesion, cysts, and combinations thereof administration of Radiopharmaceutical by Intravenous injection in hand contra lateral to breast with suspected lesion ,If bilateral lesions suspected or post bilateral mastectomy, inject in foot vein. For hand or arm injections, use IV catheter or butterfly and stopcock to avoid infiltration (very important), which may appear as false-positive axillary node uptake, Flush with at least 10 mL of saline. By using Camera with large field-of-view or dedicated scintimammography camera (SPEM: single photon emission mammographic) and Low energy with high resolution Collimator. (Williams, (2009).

#### **2.3.4. Breast Ultrasound**

Ultrasound is an adjunct to mammography and the physical examination. For palpable breast masses, it has been demonstrated that the accuracy of the combined use of US and mammography is greater than that of either used alone. For no palpable masses, by confirming the diagnosis of cysts and by providing accurate guidance for needle biopsy of the vast majority of solid masses, US contributes to the reduction of the number of surgical breast biopsies performed and aids in the early detection of cancer. Breast US is most useful in the following clinical settings: to demonstrate whether a palpable mass or a mass detected on mammography is cystic, solid or complex; to aid in the characterization of solid masses; to assess the mammographically dense breast; to assess the breast in the young, pregnant or lactating patient when ionizing radiation is contraindicated; serial follow up of a nonmalignant lesion and to evaluate the male breast. As with any test, sonography should be used to refine a differential

diagnosis only when it is needed to answer a specific diagnostic question that has been raised by the clinical history and physical examination. The image must then be integrated into patient management and correlated precisely with the other data. Although sonography can supply clues about the nature of a breast lesion, it does not reliably differentiate benign lesions and cancer. (Martin, 1999)

#### **2.3.4.1. Breast ultrasound Techniques**

**Breast Ultrasound Anatomy:** The breast is a modified sweat gland that develops between split layers of fascia. The fascial layers do not completely isolate the breast, blood vessels and lymphatics penetrate the fascial layers. The breast is composed of lobes and lobules interspersed with adipose and connective tissue {Figure 2-9}. These fat layers are heterogeneous and hypoechoic. The breast stroma is much more hyperechoic. Importantly, fat lobules contained within breast stroma can cause confusion and be misidentified as a mass lesion. Planar sheets composed of fibrous connective tissue give the breast structure. These Cooper's Ligaments are thin linear echogenic bands which ascend from the chest wall. Also within the breast tissue are the ducts which converge to form a lactiferous duct which drains each lobe. These are distinctive tubular hypoechoic structures radiating from the nipple to drain each lobule. It is this orientation which makes radial and antiradial scanning an essential component of the examination. They should be a maximum of 2mm in diameter and can usually be identified under the areolar. These drain to the lactiferous sinus (maximum 4mm.) Posterior to the main breast architecture, the pectoralis muscles can be seen as a slightly hypoechoic zone with linear strands. Anisotropy will distort the appearances of these if the scan plane is not at 90 degrees. The ribs lie posterior to this musculature and have typical attenuative properties. They are the source of confusion for those who are just commencing breast ultrasound. Another area which causes similar artifacts is the

nipple and areolar region. Compression is vital in differentiating mass from attenuating anatomy. Lymph nodes occur normally in the breast and are more predominant in the axillary region. These are often isoechoic with surrounding breast parenchyma and can be difficult to identify. Colour can be useful to detect hilar flow in a lymph node thus assisting identification. (Bassett, 1991)

Make sure the axilla is examined in both planes along with any extra mammary breast tissue. Examine the breast with the transducer parallel to the glandular/subcutaneous fat interface and with the chest wall parallel to the transducer. This allows the ultrasound beam to be perpendicular to both the superficial and deep glandular/fat interface and permits better visualization of the tissue planes. (Fornage, 1993)

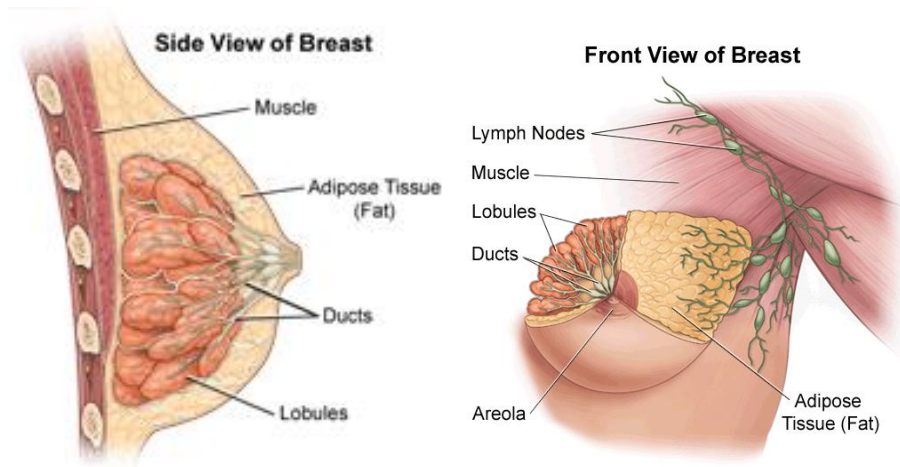


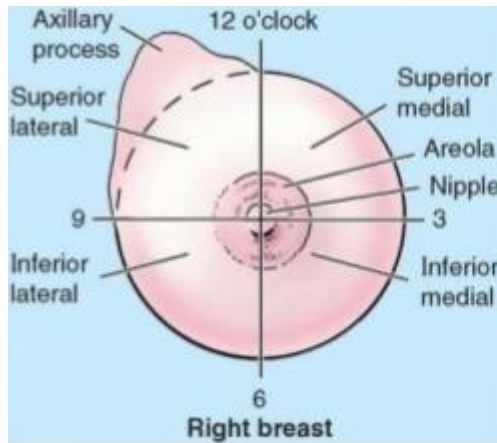
Figure (2-9 ) Anatomy of the breast

<https://www.mskcc.org/cancer-care/types/breast/anatomy-breast>

[http://www.hopkinsmedicine.org/healthlibrary/test\\_procedures/gynecology/breast\\_ultrasound\\_92](http://www.hopkinsmedicine.org/healthlibrary/test_procedures/gynecology/breast_ultrasound_92)

[,P07764/](#)

## Breast Ultrasound Technique:



1. Upper medial quadrant
2. Upper lateral quadrant
3. Lower medial quadrant
4. Lower lateral quadrant

Figure 2:10 Breast quadrants

<https://www.slideshare.net/yapa87/anatomy-of-the-breast>

Breast ultrasound is very operator dependent, the technical requirements of breast ultrasound understand of the physical principles of ultrasound and normal breast anatomy to achieve the best quality ultrasound images of the breast, a structured examination protocol. (Kopans, 1984)

**Equipment:** Breast ultrasound requires the use of high-resolution ultrasound equipment. The sonographer must select the appropriate transducer for the area to be examined. Lower frequency transducers may be required for a large breast or attenuated masses. Breast ultrasound may require the use of a stand-off. This is necessary only when the out of plane focus of the transducer is not in the region of interest. The fixed lens in front of the transducer dictates the out of plane focus. Speak to the manufacturer of equipment to determine the out of plane focus of transducers. If using 2-d arrays, control over all the focal planes and can focus the beam to the depth required. (Fornage, 1993)(Wilson, 1997). There are now varieties of high frequency probes available for breast ultrasound. The out of plane focus ranges between 0.5cm to 1.5cm to 3.5 cm

depending on the transducer. Ensure to select the probe suitable for the area you wish to image. It may be necessary to use more than one transducer to complete the examination of the breast. (Fornage, 1993).

#### **2.3.4.2. Patient Positioning**



Figure 2-11 This image demonstrate good patient position with an even distribution of breast across the chest wall

[http://www.aa.com.au/Members/soundeffectsArticles/\\_articles/BreastUltrasoundScanningTechnique%20march,%202000.pdf](http://www.aa.com.au/Members/soundeffectsArticles/_articles/BreastUltrasoundScanningTechnique%20march,%202000.pdf)

. The side to be examined is raised with the patient's hand behind their head{Figure 2-11}.The breast needs to be spread evenly across the chest wall to allow for a uniform depth of field and to reduce breast thickness. The reduced thickness allows optimization of focusing.

The degree of obliquity required varies with the size and position of the breast on the chest wall. Placing the ipsilateral hand behind the head will assist in spreading the breast further. This also allows access to the axilla. (Kopans, 1992).



### 2.3.4.3. Sonologist Positioning:



Figure 2-12 Sonographer should be comfortable during examination

<http://breastus.wikispaces.com/HOW+TO+SCAN+A+BREAST>

Position the patient close to the edge of the ultrasound couch {Figure 2-12}. Move the machine in close so that not to have stretch to reach the control panel. This will assist in reducing fatigue of the upper arm/neck etc. by decreasing the amount it is necessary to abduct the scanning arm. Invade the patient's personal space to be sufficiently close for this to be effective. The arm can be supported with a 45-degree sponge wedge. The sponge can carry the weight of the arm rather than having to hold the arm in constant abduction. It is a position that can be adopted for all scanning and can reduce some of the physical stresses of scanning. Adjustment of the height of the patient couch and the scanning chair to suit each scanning situation is also important. (Kopans, 1992)

Ultrasound Technique: There are two key components to the examination. I.e. Transverse/Para-sagittal and Radial/Antiradial. Transverse/Para-sagittal: With warm gel, examine the breast in a grid pattern in both the transverse and parasagittal plane. Overlap each scanning movement to ensure the whole breast is covered.

Consider the following guidelines from the IBUS Guidelines for the Ultrasonic Examination of the Breast. (Kopans, 1992).

### Radial/Antiradial

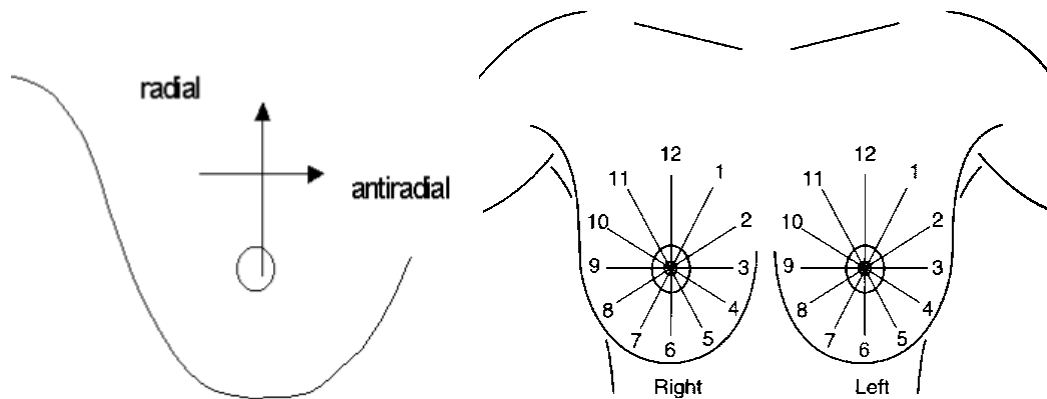


Figure 2:13 Radial/Antiradial scan planes

<http://www.aa.com.au/Members/soundeffectsArticles/articles/BreastUltrasoundScanningTechnique%20march,%202000.pdf>

Radial/Antiradial scan planes are orientated to the distribution of the ductal system (Figure 2-13). The purpose of performing this is to: Provide a scan which is reproducible, ensure the entire breast is scanned, and detect focal areas of ductal ectasia, the transducer are placed with the left margin on the nipple. The right margin is then pivoted about the nipple rotating in a clockwise direction. At 7 o'clock, the right edge is moved onto the nipple and the left edge becomes the mobile part of the transducer. (Figure 2-13)

Breast size will determine the number of rotations that are required. Once the entire clock has been scanned, any areas of concern should be reviewed in the anti-radial scan plane.

### **Patient Care:**

Patients having breast examinations require special care and attention. Patients are often well informed on breast lesion detection, management and outcomes, and can be anxious and demanding. Take care to explain to the patient the examination procedure and the process by which the patient will receive the results before starting the examination. This will hopefully avoid difficult questions from the patient at the end of the examination. (Egan, 1988)

### **2.3.4.3. Ultrasound characterization of breast parenchymal patterns:**

**Normal breast parenchymal patterns:** In the young non-lactating breast, the parenchyma is primarily composed of fibroglandular tissue, with little or no subcutaneous fat. With increasing age and parity, more and more fat gets deposited in both the subcutaneous and retromammary layers. (Howlett, 2003).

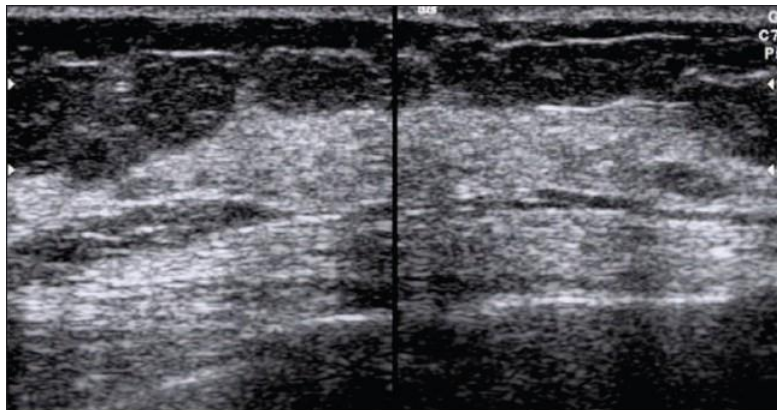


Figure : 2 -14 Normal breast. Mid transverse scan of a normal breast. The fibroglandular parenchyma is echogenic (arrowheads) and is surrounded by hypoechoic fat\*)

<http://www.ncbi.nlm.nih.gov/pmc/articles/PMC2766883/figure/F0001/>

**Breast ultrasound criteria for benign lesions:** Several studies have described the sonographic characteristics commonly seen in benign lesions of the breast: (Stavros, 1995). Smooth and well circumscribed , Hyperechoic, isoechoic or mildly hypoechoic , Thin echogenic capsule ,

Ellipsoid shape, with the maximum diameter being in the transverse plane , Three or fewer gentle lobulations, Absence of any malignant findings. (Maniero, 2005)

**Breast cysts:** are the commonest cause of breast lumps in women between 35 and 50 years of age. (Howlett,2003) .A cyst is seen on USG as a well-defined, round or oval, anechoic structure with a thin wall [Figure 2-15 A].They may be solitary or multiple [Figure 2-15 B].

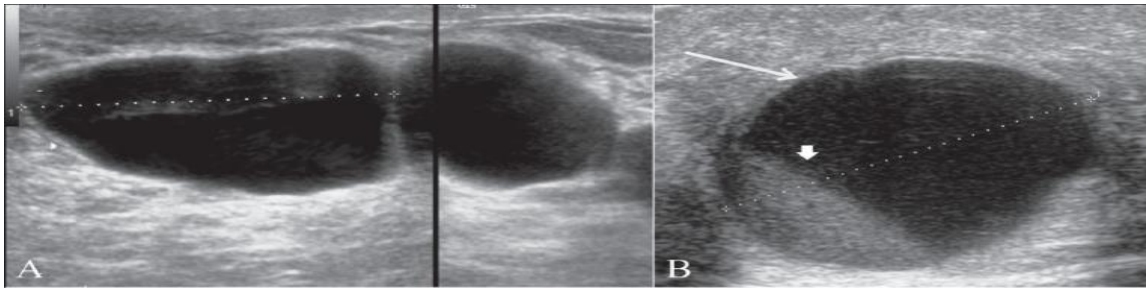


Figure: 2-15 A&B Cysts. Cysts usually reveal thin walls and through transmission (A). An inflamed cyst (B) reveals A thick edematous wall (arrow) with internal layering of thick/thin fluid (arrowhead)

<http://www.ncbi.nlm.nih.gov/pmc/articles/PMC2766883/figure/F0002/>

When internal echoes or debris are seen, the cyst is called a complex cyst. These internal echoes may be caused by floating cholesterol crystals, pus, blood or milk of calcim crystals. (Stavros, 2005). [Figure 2-15 C].

**Chronic abscess of the breast:** Patients may present with fever, pain, tenderness to touch and increased white cell count. Abscesses are most commonly located in the central or subareolar area. (Versluijs, 2002). An abscess may show an ill-defined or a well-defined outline. It may be anechoic or may reveal low-level internal echoes and posterior enhancement [Figure 2-15 D].

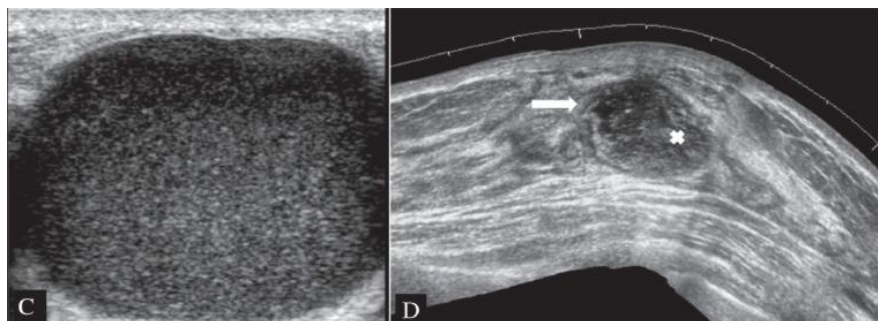
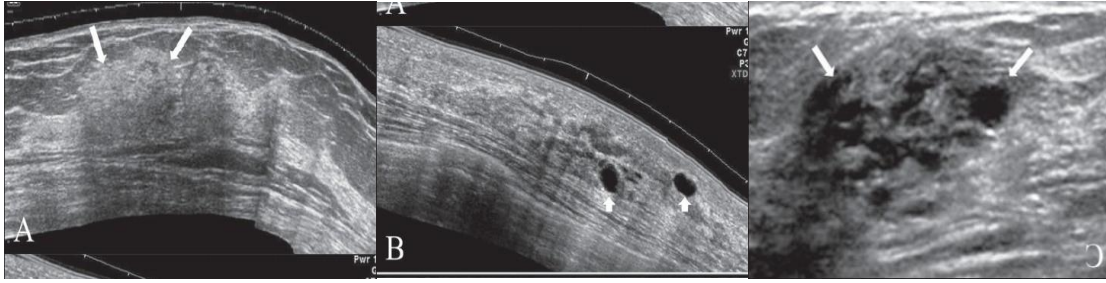


Figure: 2-15 C & D Cysts. A galactocele (C) reveals diffuse low-level echoes in the cyst.

Chronic abscess

<http://www.ncbi.nlm.nih.gov/pmc/articles/PMC2766883/figure/F0002>

**Fibrocystic breast condition:** This condition is referred to by many different names: fibrocystic disease, fibrocystic change, cystic disease, chronic cystic mastitis or mammary dysphasia. The USG appearance of the breast in this condition is extremely variable since it depends on the stage and extent of morphological changes. In the early stages, the USG appearance may be normal, even though lumps may be palpable on clinical examination. There may be focal areas of thickening of the parenchyma, with or without patchy increase in echogenicity [Figure 2- 16 A]. Discrete single cysts or clusters of small cysts may be seen in some [Figure 2-16: B, 16C]. Focal fibrocystic changes may appear as solid masses or thin-walled cysts. About half of these solid masses are usually classified as indeterminate and will eventually require a biopsy. (Shetty, 2002)



[Figure:16 A,B,C] Fibrocystic change. Extended view images (A, B) show a focal area of thickening of the breast parenchyma (A) with patchy increase in echogenicity (arrows) and scattered, discrete, thin-walled cysts (arrowheads in B). The “lump” may shows.

<http://www.ncbi.nlm.nih.gov/pmc/articles/PMC2766883/figure/F0003>

**Duct Ectasia:** This lesion has a variable appearance. Typically, duct ectasia may appear as a single tubular structure filled with fluid or sometimes may show multiple such structures as well. Old cellular debris may appear as echogenic content. If the debris fills the lumen, it can be sometimes mistaken for a solid mass, unless the tubular shape is picked up (Rizzatto, 1993).

[Figure: 2-17 A, B)

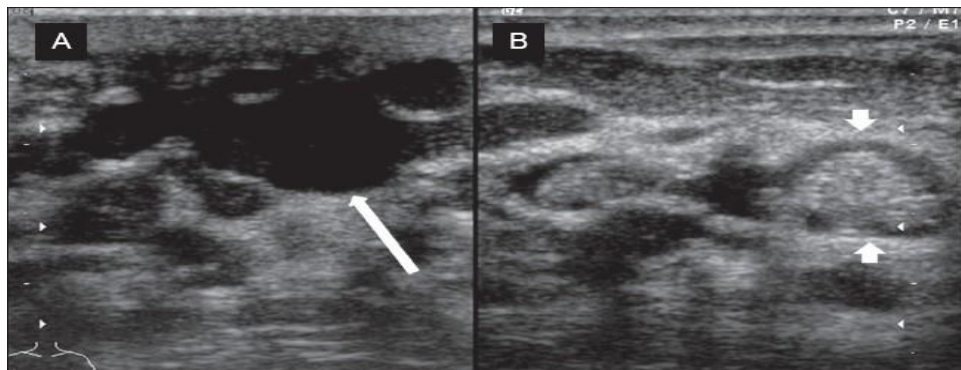


Figure 2-17 (A, B) Chronic duct ectasia. Longitudinal image (A) shows a dilated duct containing in spissated debris (arrow) is seen. In cross section (B), the intraductal debris may appear as a focal lesion (arrowheads)

<http://www.ncbi.nlm.nih.gov/pmc/articles/PMC2766883/figure/F0004>

**Fibroadenoma:** is an estrogen-induced tumor that forms in adolescence. It is the third most common breast lesion after fibrocystic disease and carcinoma. It usually presents as a firm, smooth, oval-shaped, freely movable mass. (Valea, 2007). It is rarely tender or painful. The size is usually under 5 cm, though larger fibroadenomas are known. Fibroadenomas are multiple in 10–20% and bilateral in 4% of cases. Calcifications may occur. On USG, it appears as a well-defined lesion [Figure 2-18]. A capsule can usually be identified. The echo texture is usually homogenous and hypoechoic as compared to the breast parenchyma, and there may be low-level internal echoes. Typically, the transverse diameter is greater than the anteroposterior diameter [Figure 2-18]. In a small number of patients, the mass may appear complex, hyperechoic or isoechoic. A similar USG appearance may be seen with medullary, mucinous or papillary carcinoma. (Stavros, 2004)



Figure 2-18 Fibroadenoma. Transverse image reveals a typical larger transverse than anteroposterior diameter, homogenous echo texture, and a thin capsule (arrowheads)

<http://www.ncbi.nlm.nih.gov/pmc/articles/PMC2766883/figure/F0005/>



## **2.4. Texture analysis:**

Refers to the branch of imaging science that is concerned with the description of characteristic image properties by textural features. However, there is no universally agreed-upon definition of what image texture is and in general different researchers use different definitions depending upon the particular area of application (Jain, 1998). Texture is defined as the spatial variation of pixel intensities, which is a definition that is widely used and accepted in the field. The main image processing disciplines in which texture analysis techniques are used are classification, segmentation and synthesis. In image classification the goal is to classify different images or image regions into distinct groups. Texture can be defined as a regular repetition of an element or pattern on a surface. Image textures are complex visual patterns composed of entities or regions with sub-patterns with the characteristics of brightness, color, shape, size, etc. An image region has a constant texture if a set of its characteristics are constant, slowly changing or approximately periodic. Texture can be regarded as a similarity grouping in an image. (Pietikainen, 2000)

### **2.4.1. Approach to Texture Analysis:**

Mathematical procedures to characterize texture fall into Two major categories: - Statistical and Syntactic. Statistical approaches compute different properties and are suitable if texture primitive sizes are comparable with the pixel sizes. These include Fourier transforms, convolution filters, co-occurrence matrix, spatial autocorrelation, fractals, etc. Syntactic and hybrid (Combination of statistical and syntactic) methods are suitable for textures where primitives can be described using a larger variety of properties than just tonal properties; for example shape description. Using these properties, the primitives can be identified, defined and assigned a label. For gray-level images, tone can be replaced with brightness. Statistical methods analyze the spatial



distribution of gray values, by computing local features at each point in the image, and deriving a set of statistics from the distributions of the local features. The reason behind this is the fact that the spatial distribution of gray values is one of the defining qualities of texture. Depending on the number of pixels defining the local feature, statistical method can be further classified into first order (one pixel), second-order (two pixels) and Higher-order (three or more pixels) statistics. The basic difference is that first-order statistics estimate properties (e.g. average and variance) of individual pixel values, ignoring the spatial interaction between image pixels, whereas second- and higher order statistics estimate properties of two or more pixel values occurring at specific locations relative to each other. Statistical approaches yield characterizations of textures as fine, coarse etc. Thus one measure of texture is based on the primitive size, which could be the average area of these primitives of relatively constant gray level. The average could be taken over some set of primitives to measure its texture or the average could be about any pixel in the image. If the average is taken within a primitive centered at each pixel in the image, the result can be used to produce a texture image, in which a large gray level at a pixel indicates, First order texture measures are statistics calculated from the original image values, like variance, and do not consider pixel neighborhood relationships Histogram based approach to texture analysis is based on the intensity value concentrations on all or part of an image represented as a histogram. Common features include moments such as mean, variance, dispersion, mean square value or average energy, entropy, skewness and kurtosis. Variance in the gray level in a region in the neighborhood of a pixel is a measure of the texture. (Haralick, 1979)

#### **2.4.2. First-Order Statistical Texture Analysis:**

First-order texture analysis measures use the image histogram, or pixel occurrence probability, to calculate texture. The main advantage of this approach is its simplicity through the use of

standard descriptors (e.g. mean and variance) to characterize the data (Press, 1998). However, the power of the approach for discriminating between unique textures is limited in certain applications because the method does not consider the spatial relationship, and correlation, between pixels. For any surface, or image, grey-levels are in the range  $0 \leq I \leq N_g - 1$ , where  $N_g$  is the total number of distinct grey-levels. If  $N(i)$  is the number of pixels with intensity  $i$  and  $M$  is the total number of pixels in an image, it follows that the histogram, or pixel occurrence probability, is given by:

$$P(i) = \frac{N(i)}{M}.$$

In general seven features commonly used to describe the properties of the image histogram, and therefore image texture, are computed. These are: mean; variance; coarseness; skewness; kurtosis; energy; and entropy. (Press, 1998).

### **2.4.3. Grey Level Difference Statistics Features:**

The GLDS algorithm uses first-order statistics of local property values based on the absolute differences between pairs of gray levels or of average gray levels to extract the following 5 texture measures: Homogeneity, Contrast, Mean, Energy and Entropy: Homogeneity: It is a measure of similarity in grey level intensities. Contrast: It is a measure of grey level intensity difference between neighboring pixels. Mean: It is the average value of the grey level intensities within a given area. Energy: It represents amplitude of grey level values. Entropy: It measures the randomness in grey level intensities within the given area. (Press, 1998).

#### **2.4.4. Law's texture energy measures:**

Image texture has a number of perceived qualities which play an important role in describing texture. Laws identified the following properties as playing an important role in describing texture: uniformity, density, coarseness, roughness, regularity, linearity, directionality, direction, frequency, and phase. Laws texture energy measures determine texture properties by assessing Average Gray Level, Edges, Spots, Ripples and Waves in texture. (Press, 1998).

#### **2.5. Previous study:**

Gar elnabil et.al (2011) in this study was use image-processing techniques to characterize the normal breast tissues. Clustering techniques was developed to classify the breast tissue into one of 5 different tissue types including fat, glandular, connective, dense tissues and pectoral muscle. The classification was achieved by using a novel technique involving a subset of the elements (the values on the diagonals) in the Spatial Grey Level Dependence (SGLD) matrix which was calculated using texture features, thus it was called the diagonal SGLD method (dSGLD). The ultimate goal of this study was therefore to design and implement a computerized characterization method that mimics the radiologist's characterization of tissue composition in digitized mammograms. The classification results using dSGLD and SGLD features achieved an accuracy of 80% and 71%, respectively when compared to radiologists' classifications.

M. Abdalla.et.al. (2011). studying the detection of breast tumors, there has been great attention to the modern textural features analysis of breast tissues on mammograms. Detecting of masses in digital mammogram based on second order statistics has not been investigated in depth. During this study, the breast cancer detection was based on second order statistics. The extraction of the textural features of the segmented region of interest (ROI) is done by using gray level co-occurrence matrices (GLCM) which is extracted from four spatial orientations; horizontal, left

diagonal, vertical and right diagonal corresponding to (0°, 45°, 90° and 135°) and two pixel distance for three different block size windows (8x8, 16x16 and 32x32) . The results show that the GLCM at 0°, 45°, 90° and 135° with a window size of 8X8 produces informative features to classify between masses and non-masses. Our method was able to achieve an accuracy of 91.67% sensitivity and 84.17% specificity which is comparable to what has been reported using the state-of-the-art Computer-Aided Detection system.

Sharma et.al (2013). Breast tissue density has been shown to be related to the risk of development of breast cancer, since dense breast tissue can hide lesions, causing the disease to be detected at later stages. Thus there is a need for the development of efficient techniques for the classification of breast density. In the proposed work, breast density (Fatty and Dense) is used as a pattern for classification. For carrying out the experiments mini-MIAS database has been used. This database contains images from screening mammography and has been widely used in the recent research. Texture features based on Grey Level Difference Statistics and Fourier Power Spectrum has been used for representing the texture pattern of fatty and dense mammograms. These features are then subsequently fed to the SVM classifier to classify fatty and dense mammograms. The results show that the extracted features perform very well with Polynomial Kernel of Support Vector Machine (SVM) classifier giving an accuracy of 97.25%. The experimental results encourage the use of proposed method for the classification of breast density.

Shi et al. (2008) this study was to develop an automated method for mammographic mass segmentation and explore new image based features in combination with patient information in order to improve the performance of mass characterization. Previous CAD system, which used the active contour segmentation, and morphological, textural, and speculation features, has

achieved promising results in mass characterization. The new CAD system is based on the level set method, and includes two new types of image features related to the presence of micro calcifications with the mass and abruptness of the mass margin, and patient age. A linear discriminate analysis (LDA) classifier with stepwise feature selection was used to merge the extracted features into a classification score. The classification accuracy was evaluated using the area under the receiver operating characteristic curve. Our primary data set consisted of 427 biopsy-proven masses (200 malignant and 227 benign) in 909 regions of interest (ROIs) (451 malignant and 458 benign) from multiple mammographic views. Leave-one-case-out resembling was used for training and testing. The new CAD system based on the level set segmentation and the new mammographic feature space achieved a view-based as value of  $0.83\pm 0.01$ . The improvement compared to the previous CAD system was statistically significant ( $p=0.02$ ). When patient age was included in the new CAD system, view-based and case based as values were  $0.85\pm 0.01$  and  $0.87\pm 0.02$ , respectively. The performance of the new CAD system was also compared to an experienced radiologist's likelihood of malignancy rating. When patient age was used in classification, the accuracy of the new CAD system was comparable to that of the radiologist ( $p=0.34$ ). The study also demonstrated the consistency of the newly developed CAD system by evaluating the statistics of the weights of the LDA classifiers in leave one-case-out classification. Finally, an independent test on the publicly available digital database for screening mammography (DDSM) with 132 benign and 197 malignant ROIs containing masses achieved a view-based as value of  $0.84\pm 0.02$ .

Moon et al. (2015) develop a computer-aided diagnosis (CAD) system based on texture features for distinguishing between TNBC and benign fibroadenomas in US images. US images of 169 pathology-proven tumors (mean size, 1.65 cm; range, 0.7-3.0 cm) composed of 84 benign

fibroadenomas and 85 TNBC tumors are used in this study. After a tumor is segmented out using the level-set method, morphological, conventional texture, and multi resolution gray-scale invariant texture feature sets are computed using a best-fitting ellipse, gray-level co-occurrence matrices, and the ranklet transform, respectively. The linear support vector machine with leave-one-out cross-validation schema is used as a classifier, and the diagnostic performance is assessed with receiver operating characteristic curve analysis. The Az values of the morphology, conventional texture, and multi resolution gray-scale invariant texture feature sets are 0.8470 [95% confidence intervals (CIs), 0.7826-0.8973], 0.8542 (95% CI, 0.7911-0.9030), and 0.9695 (95% CI, 0.9376-0.9865), respectively. The Az of the CAD system based on the combined feature sets is 0.9702 (95% CI, 0.9334-0.9882). and his study conclude that, the CAD system based on texture features extracted via the ranklet transform may be useful for improving the ability to discriminate between TNBC and benign Fibroadenoma.

LIAO et.al (2011) stated that benign and malignant tumors can be classified by using texture analysis of ultrasound B-scan image to describe the variation in the echogenicity of scatterers. The recently proposed ultrasonic Nakagami parametric image has also been used to detect the concentrations and arrangements of scatterers for tumor characterization applications. B-scan based texture analysis and the Nakagami parametric image are functionally complementary in ultrasonic tissue characterizations and this study aimed to combine these methods in order to improve the ability to characterize breast tumors by using radio-frequency data obtained from 130 clinical cases were used to construct the texture-feature parametric image and the Nakagami parametric image. Four texture-feature parameters based on a gray-level co-occurrence matrix (homogeneity, contrast, energy, and variance) and the Nakagami parameters of the benign and malignant tumors were calculated. The usefulness of an individual parameter was determined

and scatter graphs indicated the relationship between two selected texture-feature parameters. Fisher's linear discriminant analysis was used to combine the selected texture-feature parameters with the Nakagami parameter. The performance in classifying tumors was evaluated based on the receiver operating characteristic curve, then results indicated that there is a trade-off between sensitivity and specificity when using an individual texture-feature parameter or when combining two such correlated parameters to discriminate benign and malignant cases. However, the best performance was obtained when combining selected texture-feature parameters with the Nakagami parameter. The study findings suggest that combining B-scan-based texture analysis and the Nakagami parametric image could improve the ability to classify benign and malignant breast tumors.

Huber et.al (2010) was aimed to evaluate the differential diagnostic value of a method of computer-assisted texture analysis in comparison to established Ultrasonographic B-mode characteristics in the examination of solid breast masses. At two centers, 77 patients presenting with a solid mass on B-mode scan were studied at 7.5 MHz. Description of B-mode appearance included assessment of tumor shape, borders, presence of an echogenic rim, tissue architecture, internal echo structure, absorption and elasticity. For statistical pattern recognition, the following parameters were used: form factor, mean grey level, signal-to-noise ratio, and mean gradient and correlation from the co-occurrence matrix. At center 1, the most decisive parameter for differential diagnosis was distortion of tissue architecture (sensitivity, SN, 83%; specificity, SP, 92%) and, at center 2, relation to the adjacent tissue (SN 93%, SP 92%). Among texture parameters, best discrimination was achieved for correlation from the co-occurrence matrix at center 1 (SN 58%, SP 73%) and for form factor at center 2 (SN 93%, SP 77%). Among sonographic criteria, the highest contribution to the diagnosis was found for an un sharp border

(odds ratio, OR, 12.2), architectural distortion (OR, 8.6), fixation to skin or chest wall (OR, 9.0) and fixation to adjacent breast parenchyma (OR, 8.8), according to texture analysis for parameters form factor (OR 4.0) and correlation from the co-occurrence matrix (OR 4.7). Concluded that Ultrasonographic texture analysis can be helpful as an additional parameter in differential diagnosis of breast tumors, but did not reach differential diagnostic accuracy of sonomorphologic features.

Boukerroui et.al (1998) was examined a specific algorithm which is presented for the automatic extraction of breast tumors in ultrasonic imaging , by involves two-dimensional adaptive K-means clustering of the gray scale and textural feature images. The segmentation problem is formulated as a maximum a posteriori (MAP) estimation problem. The MAP estimation is achieved using Besag's iterated conditional modes algorithm for the minimization of an energy function. This function has three components: the first constrains the region to be close to the data; the second imposes spatial continuity; and the third takes into consideration the texture of the various regions. A multi-resolution implementation of the algorithm is performed using a wave less basis; Experiments were carried out on synthetic images and on in vivo breast ultrasound images. Various parameters involved in the algorithm are discussed to evaluate the robustness and accuracy of the segmentation method Then concluded that textural features in the segmentation of ultrasonic data improves the robustness of the algorithm and makes the segmentation result less parameter dependent.

Skaane et.al (1998) was determined the predictive power of sonographic tumor descriptors in the differentiation of Fibroadenoma from invasive ductal carcinoma of the breast. By using three hundred thirty-six tumors (142 fibroadenomas and 194 invasive ductal carcinomas) of the breast diagnosed using sonography were prospectively recorded with respect to the shape, contour,



echo texture, echogenicity, sound transmission, and surrounding tissue of the tumors. Evaluation included odds and odds ratios of single sonographic features as well as sensitivity, specificity, and positive and negative predictive values of combinations of features. Tumor descriptors were also evaluated using multiple logistic regression analysis after adjustment for age and clinical examination. Then resulting as that , Irregular shape and contour, extensive hypoechogenicity, shadowing, echogenic halo, and distortion of surrounding tissue were the findings with the highest predictive value of malignancy. A thin echogenic pseudo capsule was the most important sonographic finding predictive of the benign nature of a solid mass. Echo texture was of little value in the differentiation of breast tumors. Age and clinical examination remained important predictors in a clinically referred patient population because a palpable mass in an elderly patient is most likely a carcinoma. We saw considerable overlap of most sonographic features in both benign and malignant tumors. However, using strict sonographic criteria and a combination of descriptors, we found a negative predictive value of 100% in palpable and 96% in impalpable tumors. Concluded A combination of tumor descriptors gave negative predictive values approaching 100%, allowing downgrading of solid breast masses with a high degree of confidence. Extensive sonographic features analysis in patients with indeterminate clinical and mammographic findings has the potential for downgrading a tumor and possibly obviating the need for excision in a subgroup of patients. Further investigations may provide standardization of sonographic descriptor analysis and establishment of the combination of the most predictive features that would be useful in daily practice.

Cai L et.al (2015) was described; Classification of breast ultrasound (BUS) images is an important step in the computer-aided diagnosis (CAD) system for breast cancer. In this paper, a novel phase-based texture descriptor is proposed for efficient and robust classifiers to

discriminate benign and malignant tumors in BUS images. By descriptor, namely the phased congruency-based binary pattern (PCBP) is an oriented local texture descriptor that combines the phase congruency (PC) approach with the local binary pattern (LBP). The support vector machine (SVM) is further applied for the tumor classification. To verify the efficiency of the proposed PCBP texture descriptor, we compare the PCBP with other three state-of-art texture descriptors, and experiments are carried out on a BUS image database including 138 cases. The receiver operating characteristic (ROC) analysis is firstly performed and seven criteria are utilized to evaluate the classification performance using different texture descriptors. Then, in order to verify the robustness of the PCBP against illumination variations, we train the SVM classifier on texture features obtained from the original BUS images, and use this classifier to deal with the texture features extracted from BUS images with different illumination conditions (i.e., contrast-improved, gamma-corrected and histogram-equalized). The area under ROC curve (AUC) index is used as the figure of merit to evaluate the classification performances. He concluded that the proposed PCBP texture descriptor achieves the highest values (i.e. 0.894) and the least variations in respect of the AUC index, regardless of the gray-scale variations. It's revealed in the experimental results that classifications of BUS images with the proposed PCBP texture descriptor are efficient and robust, which may be potentially useful for breast ultrasound Cads.

Fornage et.al (1989) described the sonographic appearance of breast fibroadenomas, He examined patterns of 100 fibroadenomas, including two giant fibroadenomas and two cyst sarcoma phyllodes, were reviewed. The lesions were mostly hypoechoic (92%) and homogeneous in echotexture (72%). Twenty-seven percent of fibroadenomas showed irregular margins. Intratumoral calcifications were noted in 10% of lesions. A marked acoustic shadow

without associated calcification was seen in six cases. The mean ratio of the length to the anteroposterior diameter of the tumors was 1.84 +/- 0.52 (standard deviation), indicating an elongation along the general orientation of the breast tissue planes. The ratios of length to anteroposterior diameter calculated in two matching groups of small (less than 1 cm<sup>3</sup>) fibroadenomas and carcinomas differed significantly. State-of-the-art high-frequency transducers, geometric analysis of tumors, and real-time ultrasound-guided fine-needle aspiration biopsy should help to distinguish between benign and malignant solid breast masses.

Jung et al. (2014) studied and evaluate the sonographic appearance and characteristic feature of juvenile Fibroadenoma of the breast. On sonography, all fibroadenomas presented as masses. The mean size was 30 mm. regarding shape, there were 29 oval, 2 round, and 3 irregular masses. The margins were circumscribed in 24, indistinct in 5, micro lobulated in 4, and angular in 1. Regarding echogenicity, 16 masses were hypoechoic, 16 isoechoic, and 2 complexes echoic. Posterior acoustic characteristics included posterior acoustic enhancement in 22 masses (65%), posterior shadowing in 1, and no posterior acoustic features in 9; this information was not available in 2. The lesion boundary presented as an abrupt interface in 32 and an echogenic halo in 2. The orientation was parallel in 32 and nonparallel in 2. Calcifications were present in 3 cases and absent in 31. On color Doppler sonography, the masses were usually hyper vascular with vessel counts of 5 or more (87%). The BI-RADS final assessment categories were 3 in 24 and 4a in 10. He concluded that the dominant sonographic presentation of juvenile Fibroadenoma is a circumscribed oval hypoechoic or isoechoic mass, which resembles that of simple Fibroadenoma. Juvenile fibroadenomas frequently show posterior acoustic enhancement and hyper vascularity on color Doppler sonography.

Strano et.al (2004) aimed to evaluate color Doppler imaging of fibroadenomas of the breast with histopathological correlation, the study was aimed to conduct and characterize the spatial distribution of blood vessels in breast fibroadenomas. We performed a prospective study to map the anatomic distribution of the vessels in 29 fibroadenomas of the breast using color Doppler sonography. We categorized the detected vessels according to their location in or on the fibroadenoma, counted the different types of vessels, and tested for correlations between vessel distributions or numbers and histopathologic findings. Blood flow was demonstrated in 24/29 (83%) of fibroadenomas. We found 3 vessel types: feeding vessels, which are prominent vessels leading from the surrounding breast tissue into the fibroadenomas; capsular vessels, which are located within the tissue capsule; and segmental vessels, which are located within the fibrous septa of the fibroadenoma. Capsular and segmental vessels were demonstrated in 23/24 (96%) and 24/24 (100%) of the cases, respectively. Feeding vessels were seen in 12/24 (50%) of the cases. Histopathologic analysis revealed the same location and distribution of the vessels as color Doppler imaging. However, there was no correlation between numbers of vessels counted on sonograms and on histopathologic specimens, the study concluded that, examination of the vascularity demonstrated on color Doppler imaging helps in the diagnosis of benign breast neoplasms such as fibroadenomas.

Rothschild et.al (1886) aimed to evaluate the spectrum of sonographic findings of fibroadenoma of the breast; there are a number of sonographic findings seen in fibroadenoma of the breast. In a retrospective study, we examined the biopsy results of 59 masses given the sonographic diagnosis of fibroadenoma. We also reviewed the sonograms of an additional 26 biopsy-proven fibroadenomas that were not diagnosed as such with ultrasound. The ultrasound diagnosis was correct in 50 of 76 fibroadenomas (65.8%). Only 12 of the 76 biopsy-proven fibroadenomas had

the classic sonographic appearance of a smooth round or oval mass with homogeneous internal echoes. Fourteen fibroadenomas were not visible on the sonograms, even in retrospect. The remaining 50 biopsy-proven fibroadenomas demonstrated one or more "atypical" signs of border irregularity, lobulation, inhomogeneous internal echo texture, or posterior shadowing. There were nine sonographic false positives: five patients had other benign lesions on histology, and four masses believed to be sonographically compatible with fibroadenoma were found to be carcinomas. While breast sonography is frequently a useful modality for breast mass detection, particularly as an adjunct to x-ray mammography, the common overlap in characteristics of benign and malignant masses makes histologic evaluation of all solid masses essential.

Soriano et.al (1983) evaluated breast fibroadenoma sonomammography correlated with pathology, during the performance of 2,000 sonomammograms; there were 122 patients with 140 biopsy-confirmed fibroadenomas. Mass lesions or abnormalities were detected on the sonomammograms in 100 of these patients (82%) (118/140 masses), and a retrospective review of the descriptive sonographic criteria tabulated at the initial interpretation of 118 of these masses was undertaken. The most significant sonographic mass features were a round (48%) or oval (37%) shape, a smooth contour (75%), weak internal echoes (80%) in a uniform distribution (88%), and intermediate acoustic attenuation (71%). A pathologist reviewed all the cases, tabulating the gross and microscopic appearance of each specimen. In addition, the average fibrous and epithelial tissue content of 103 tumors (100 fibroadenomas and three adeno fibromas) was recorded from a review of five low-power microscopic fields of representative areas of the tumor and correlated with the sonographic features. The sonomammographic features of seven calcified fibroadenomas, five giant fibroadenomas, and one fibroadenoma

containing in situ lobular carcinoma and a subgroup having both sonomammograms and radiomammograms are discussed.

## Chapter three

### Material and Methods

#### 3.1 Ultrasound machine:

Breast ultrasound examination was performed with Siemens ultrasound machines with high frequency linear 10 MHz probe is typically used to scan the breast.



Figure.3.1 an acoustic coupling agent, "gel"



Figure.3.2 Linear array probe 10 MHz

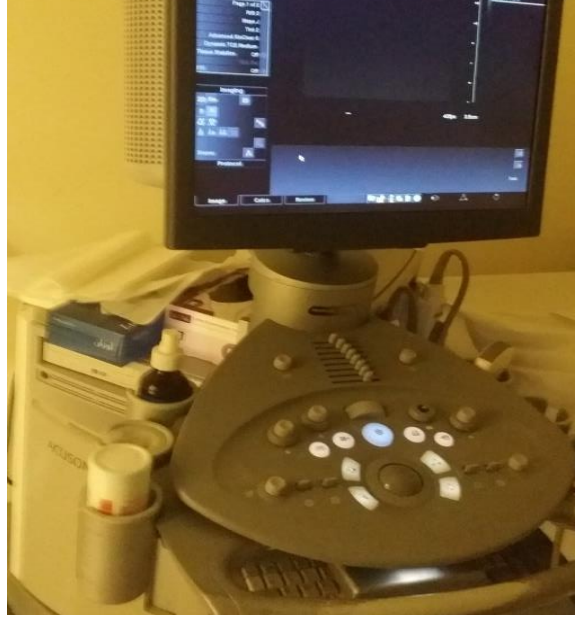


Figure 3.3 Siemens Ultrasound unit

### 3.2. Methods:

Patient was selected according to the study variability and ultrasound imaging was performed for three group of patient which those with breast lump (Fibroadenoma) after confirmation by biopsy and those having feature of breast cyst and then all these patient compared to the normal breast tissue in ultrasound exam, firstly the lesion was characterized using the ordinary US feature like echogenicity and others, after that US images were stored in computer disk were viewed by the Radiant, Ant DICOM Digital imaging and communication on medical in computer to selected the coronal images that suit the criteria of research population then uploaded into the computer based software Interactive Data Language (IDL) where the DICOM image converted to TIFF format to suit IDL platform. Then the image were read by IDL in TIFF format and textural features that represent the first order were extracted from the Breast tissue from the three groups which are the Fibroadenoma, breast fibroglandular tissue and Cystic changes in breast, these features include mean, standard deviation, signal to noise ratio, energy and entropy using a window of  $3 \times 3$  pixel from all data set using breast and as Region of Interest (ROI) through an



algorithm written in Interactive Data Language (IDL) software. The extracted features were classified using stepwise linear discriminant analysis using breast as separate data set where each include the previous three groups; in order to find the most discriminant textural feature in each set as well as the classification accuracy and sensitivity concerning the characteristics of each set.

### **3.2.1. Technique**

The breast should be assessed into radial or anti/radial plane. Using a warm gel, examine the breast in a pattern in both transverse and para-sagittal plane. Overlap each scanning movement to ensure the whole breast is covered. The transducer is placed with the left margin on the nipple. The right margin is then pivoted about the nipple rotating in a clockwise direction. At 7 o'clock, the right edge is moved onto the nipple and the left edge becomes the mobile part of the transducer.

### **3.2.2. Design of the study:**

This study is analytical-case control type deals with Sonographic pattern of breast Fibroadenoma.

### **3.2.3. Population of the study:**

The population of this study consisted of two groups of patient, those with normal breast free from any mass as control group, group two patients diagnosed as having breast Fibroadenoma. The study includes both genders with their age ranged from 16 years to 80years old.

### **3.2.4. Sample size and type:**

This study consisted of 130 patients having breast ultrasound examination, referred to ultrasound department for scanning. Patients were selected conveniently.

### **3.2.5. Place and Duration of the study:**

This study was carried out in the period from September 2013 to August 2016 in Saad specialist hospital. K.S.A.

### **3.2.6. Inclusion criteria:**

All patients diagnosed with Fibroadenoma and cyst or those with benign breast lump

### **3.2.7. Exclusion criteria:**

All patients with malignant transformation and those having other breast disease and other breast masses were excluded from this study.

### **Methods of data collection:**

The data was collected by using slandered master data sheet used for collection of the study variable

### **Methods of data analysis:**

Data analysis methods calcified into two categories, first one concern with US/characterization and the other one with image texture analysis. Where the data were analyzed using SW-LDA in SPSS and excels Microsoft office was also used.

### **Ethical approval:**

The ethical approval was granted from the hospital and the radiology departments; which include commitment of no disclose any information concerning the patient identification as well as consent from the patients.

## Chapter Four

### Result

Ultrasound scanning was performed in the Ultrasound Unit of Saad specialist Hospital in KSA.

The data was collected from 130 women complaining of breast disease mostly related to be fibroadenoma or cystic changes in which normal patient was also taken.

Age, echogenicity, texture, breast related variables was measured in addition to the breast texture from FOS was also extracted in order to compare texture analysis to normal ultrasound characterization. The mean age was 41.8 years in all patients. (Table 4-1). Detailed results are shown in the tables and figures below.

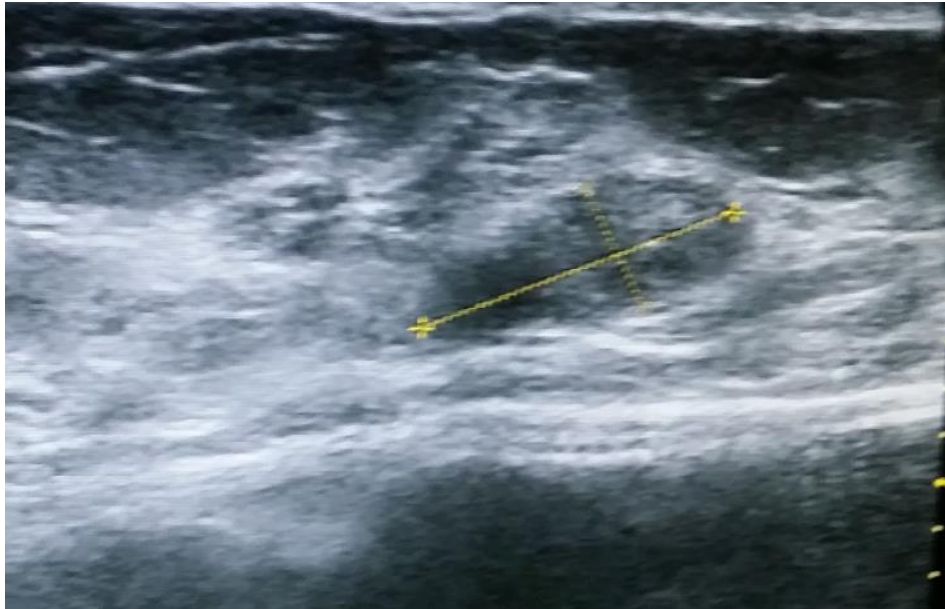


Figure (4.1) original ultrasound images for breast fibroadenoma

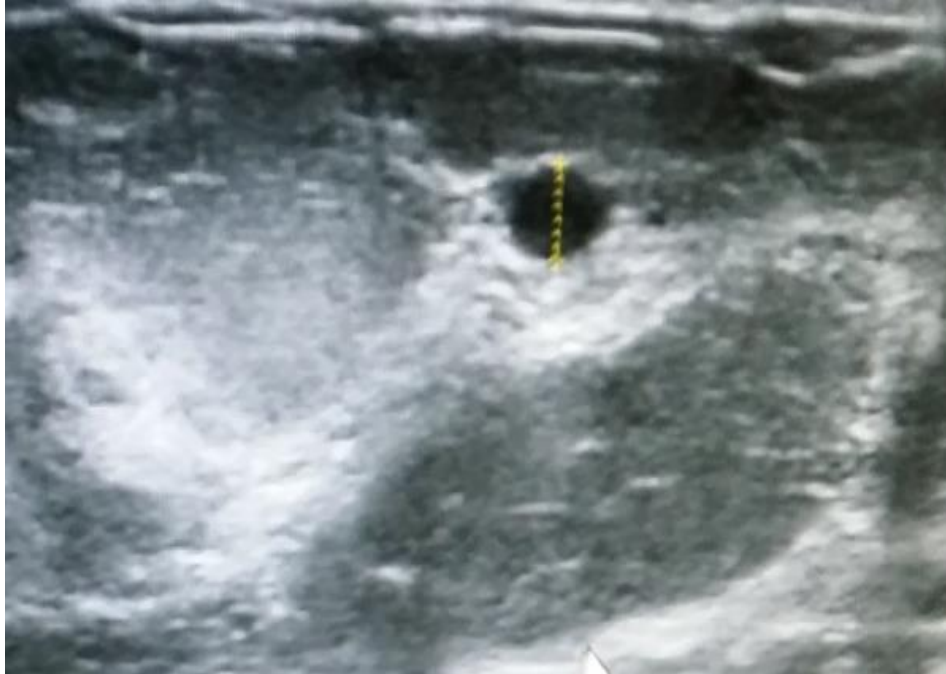


Figure (4.2) original image of breast cyst in U/S.

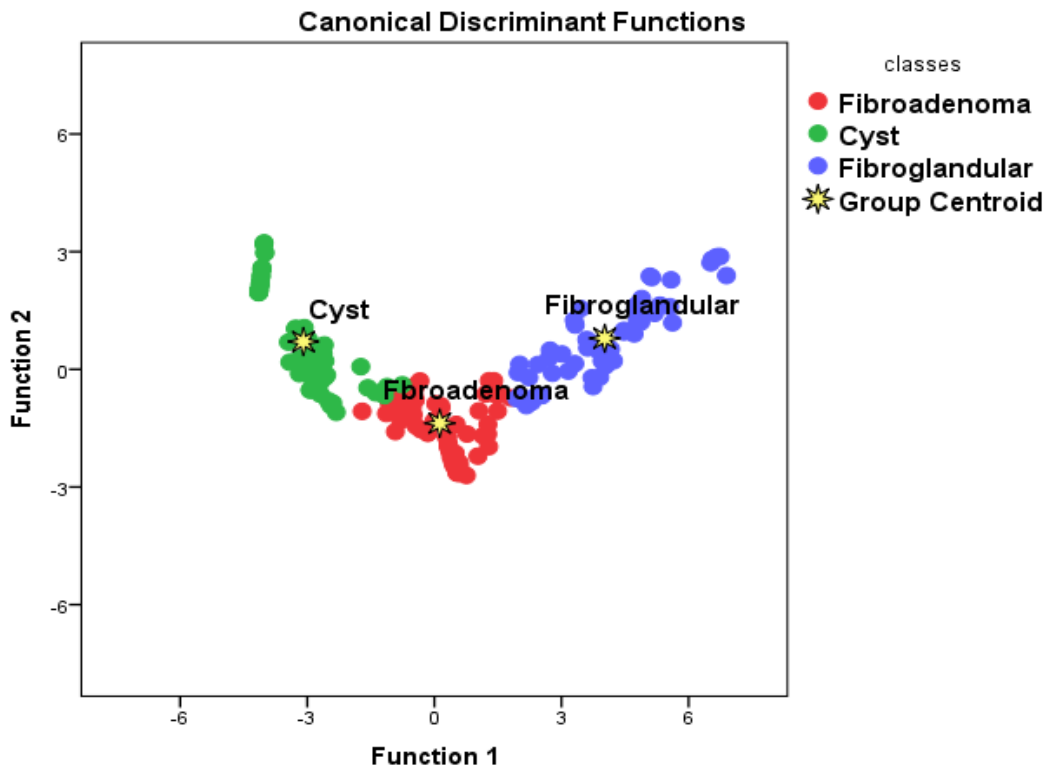


Figure (4.3): Scatter plot generated using discriminate analysis function for three classes represents: Fibroadenoma, cyst and normal fibroglandular tissue.

Table 4.1: Showed the classification accuracy of the Fibroadenoma using linear discriminant analysis:

Classes		Predicted Group Membership			Total
		Fibro-adenoma	Cyst	Fibro-glandular	
Original	Fibro-adenoma	<u>100.0</u>	0.0	0.0	100.0%
	Cyst	7.2	<u>92.8</u>	0.0	100.0%
	Fibro-glandular	7.8	0.0	<u>92.2</u>	100.0%

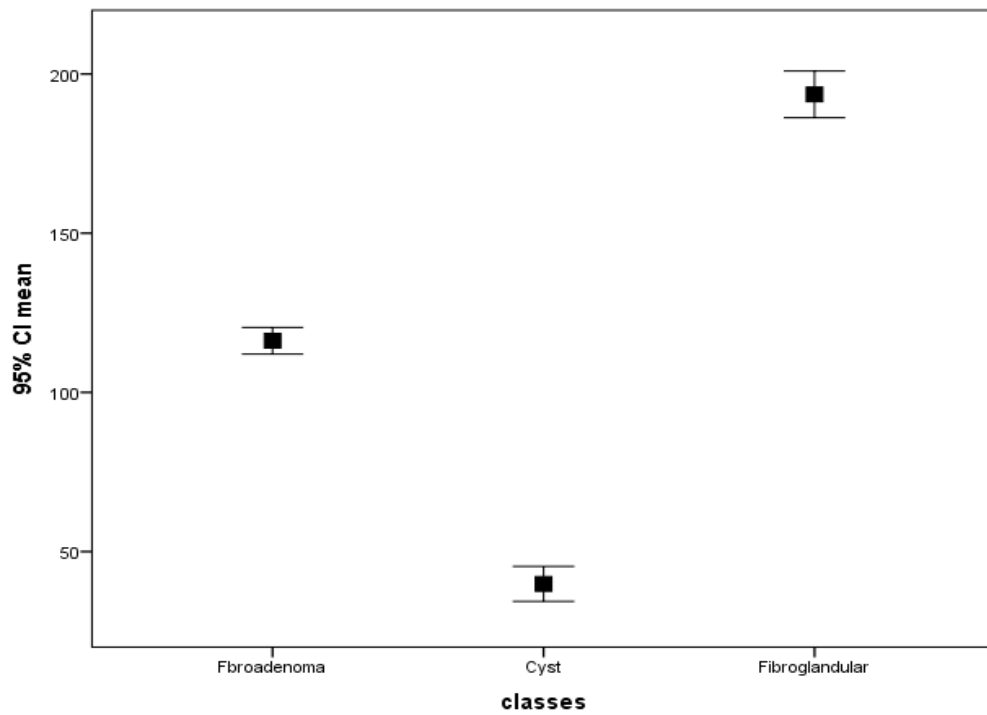


Figure (4.4). Classification based on mean feature for breast US.

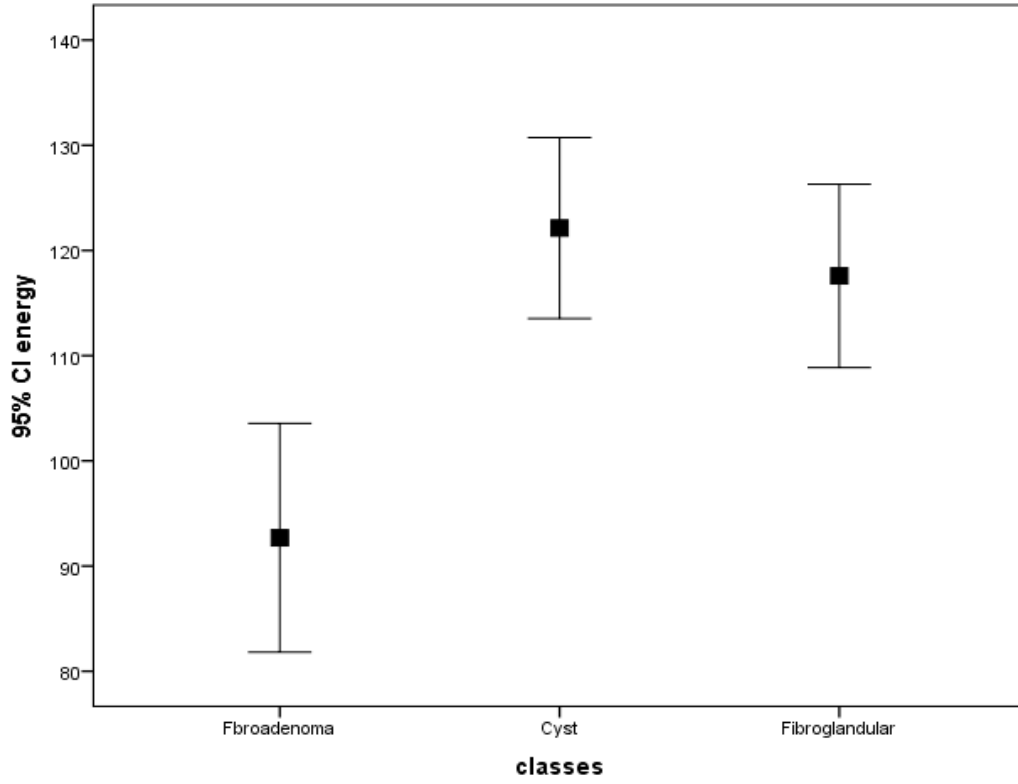


Figure (4.5). Classification based on energy feature for breast US.

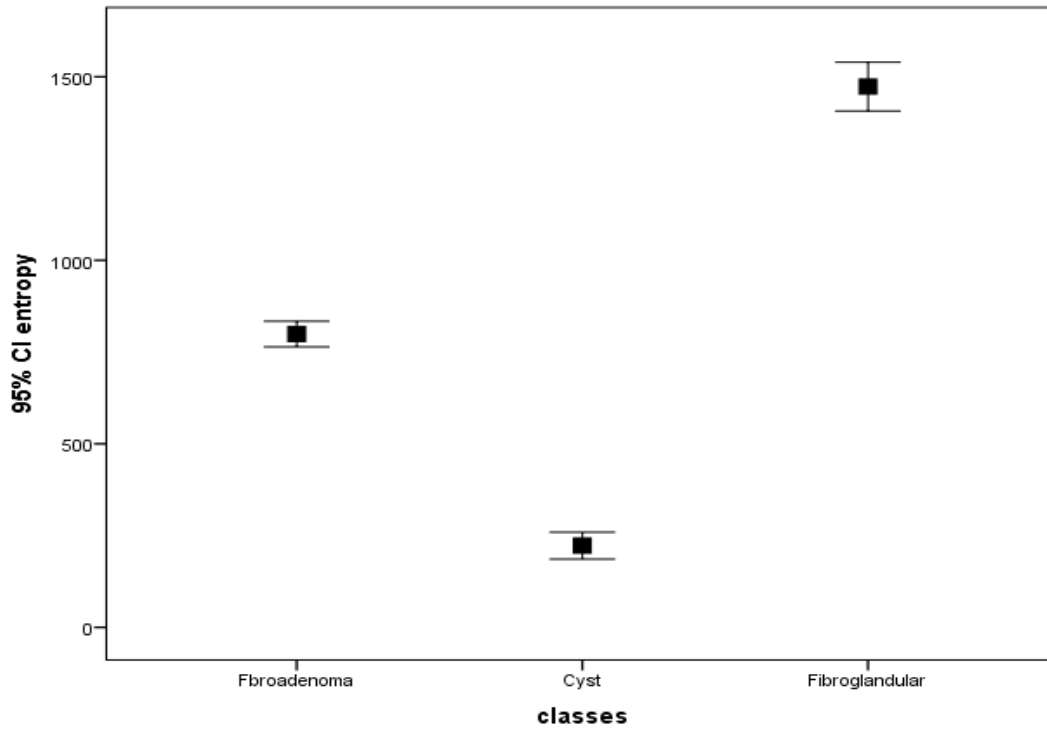


Figure (4.6). Classification based on entropy feature for breast US.

Table 4.2. Showed the statistics of patient related variables (mass size (0) indicate the normal cases)

	Minimum	Maximum	Mean	Std. Deviation
Age	16	75	41.81	13.146
Weight	47	108	73.96	13.647
Height	110	170	156.92	7.745

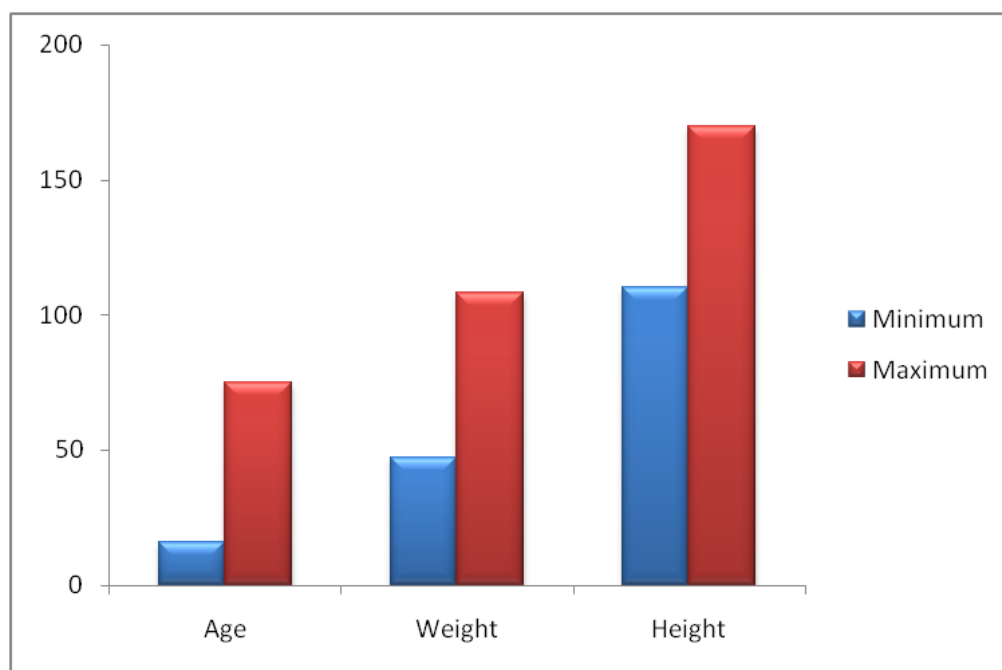


Figure 4.7 Bar graph of a cross tabulation showed the relation between (mass size (0) indicate normal cases)

Table 4.3. Showed the relation between maternal status and site of the Lesion

Maternal status		Site			Total
		Normal	Rt	Lt	
Maternal status	Single	8	4	7	19
	Married	32	38	41	111
Total		40	42	48	130
Correlation is significant at $P < 0.05$ , $p = 0.448$					

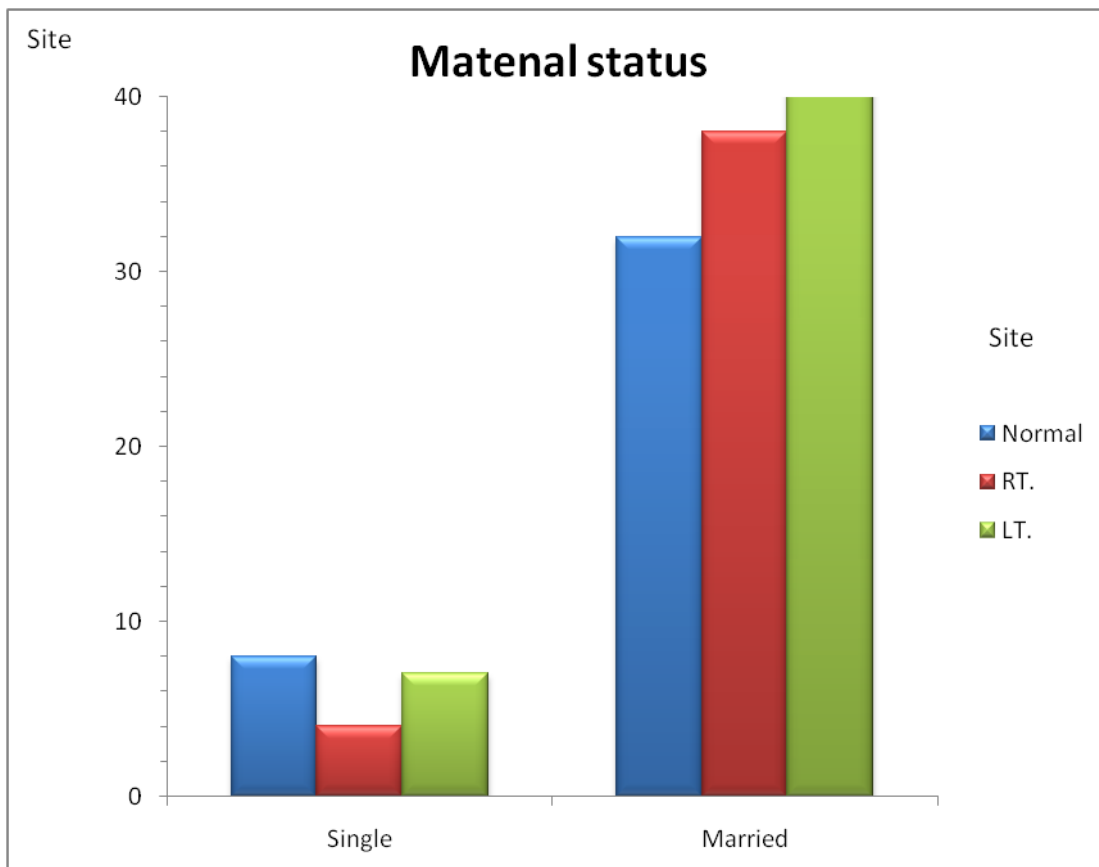


Figure (4.8). Bar graph of a cross tabulation showed the relation between maternal status and lesion site



Table 4.4. Showed the relation between the maternal status and Lesion echo texture

		Texture			Total
		No lesion	Homogenous	Heterogeneous	
Maternal status	Single	8	6	5	19
	Married	32	60	19	111
Total		40	66	24	130
Correlation is significant at $P < 0.05$ , $p = 0.431$					

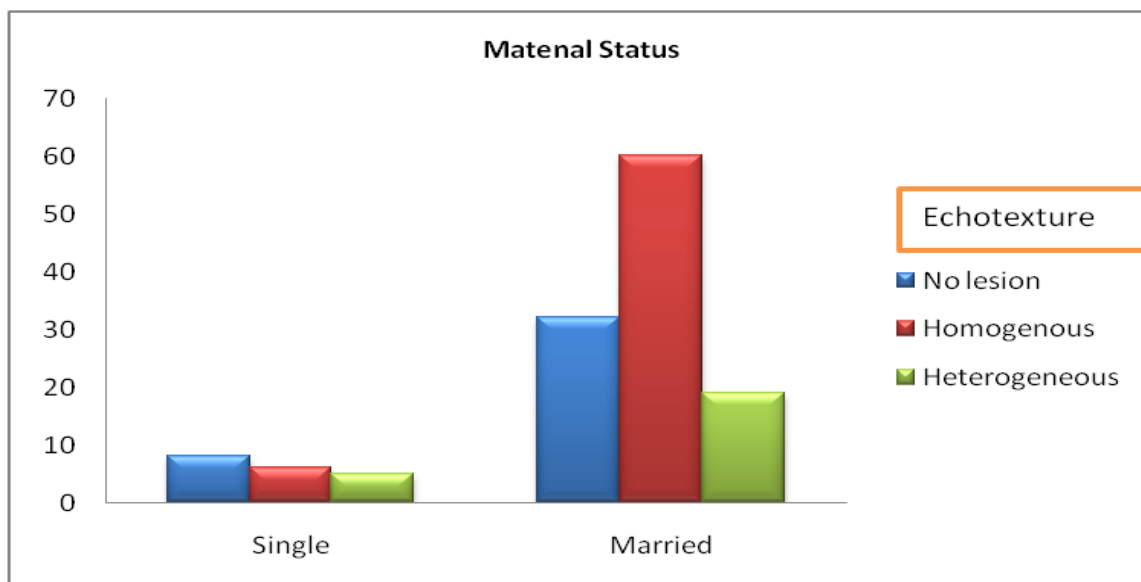
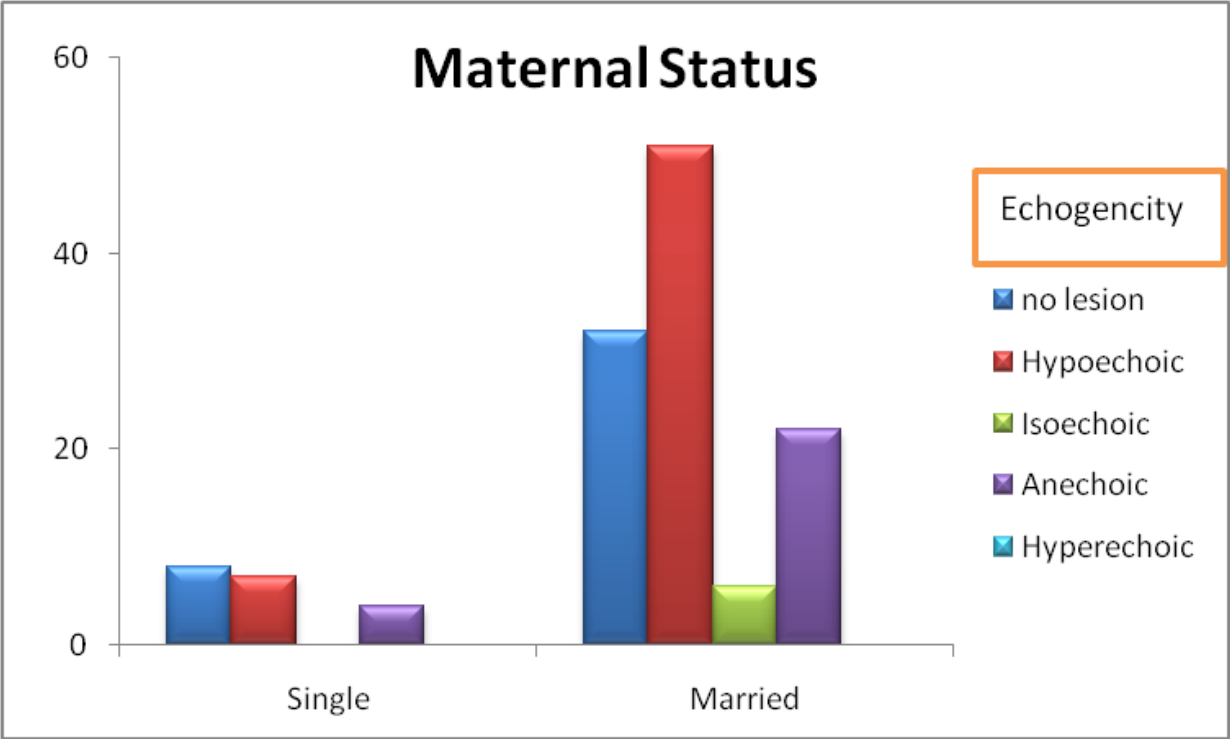


Figure (4.9) Bar graph showed cross tabulation showed the relation between the maternal status and lesion echotexture .

Table 4.5. Cross tabulation showed the relation between maternal status and lesion Echogensity

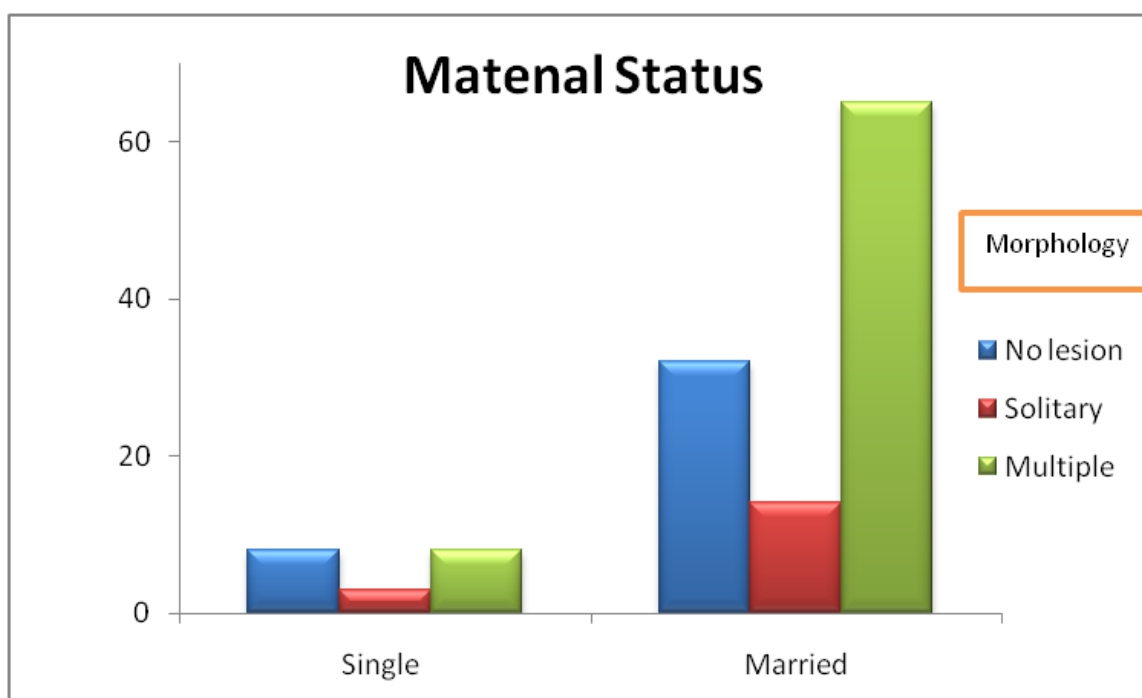
		Echogensity					Total
		no lesion	Hypoechoic	Isoechoic	Anechoic	Hyperechoic	
Maternal status	Single	8	7	0	4	0	19
	Married	32	51	6	22	0	111
Total		40	58	6	26	0	130
Correlation is significant at $P < 0.05$ , $p = 0.901$							



Figure(4.10).Cross tabulation showed the relation between maternal status and lesion Echogensity

Table 4.6. Cross tabulation showed the relation between maternal status and lesion morphology

		Morphology			Total
		no lesion	Solitary	Multiple	
Maternal status	Single	8	3	8	19
	Married	32	14	65	111
Total		40	17	73	130
Correlation is significant at $P < 0.05$ , $p = 0.937$					



Table(4.11). Cross tabulation showed the relation between maternal status and lesion morphology

Table 4.7. Cross tabulation showed the relation between maternal status and lymphadenopathy

		Lymph node		Total
		Normal	Presence of LN	
Maternal status	Single	16	3	19
	Married	94	17	111
Total		110	20	130
Correlation is significant at $P < 0.05$ , $p = 0.753$				

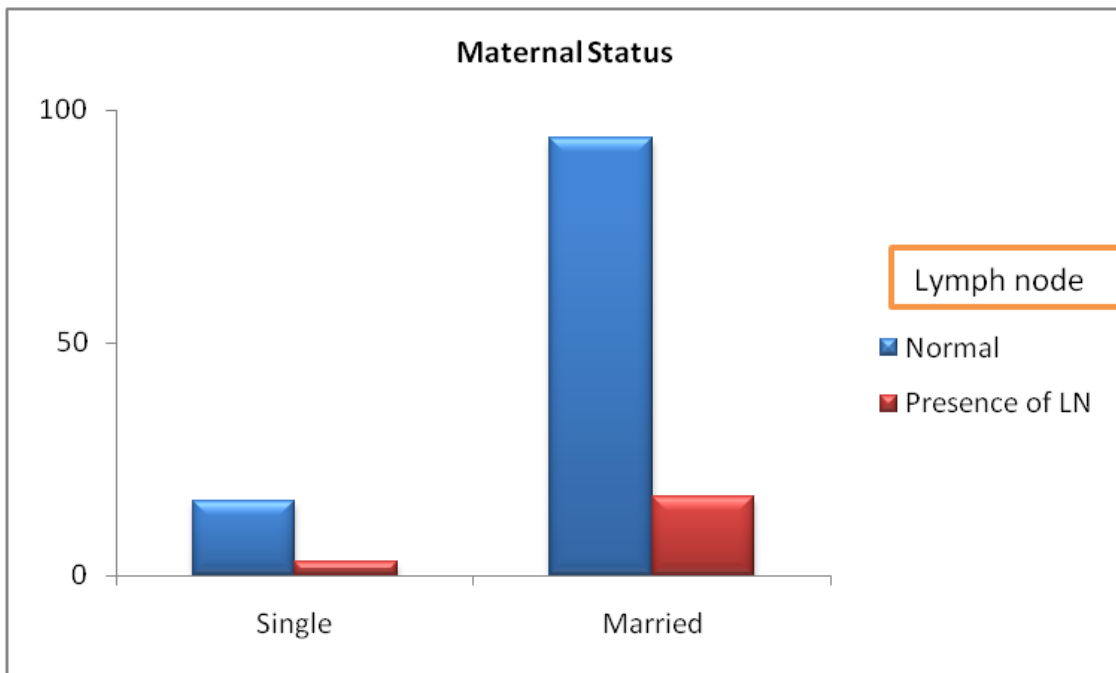


Figure (4.12). Cross tabulation showed the relation between the maternal status and the lymphadenopathy of the disease

Table 4.8. Cross tabulation showed the relation between the menstrual cycle and lesion echo texture

		Texture			Total
		No lesion	Homogenous	Heterogeneous	
menstrual cycle	Regular	18	26	10	54
	Irregular	8	18	8	34
	Menopause	14	22	6	42
Total		40	66	24	130

Correlation is significant at  $P < 0.05$ ,  $p = 0.564$

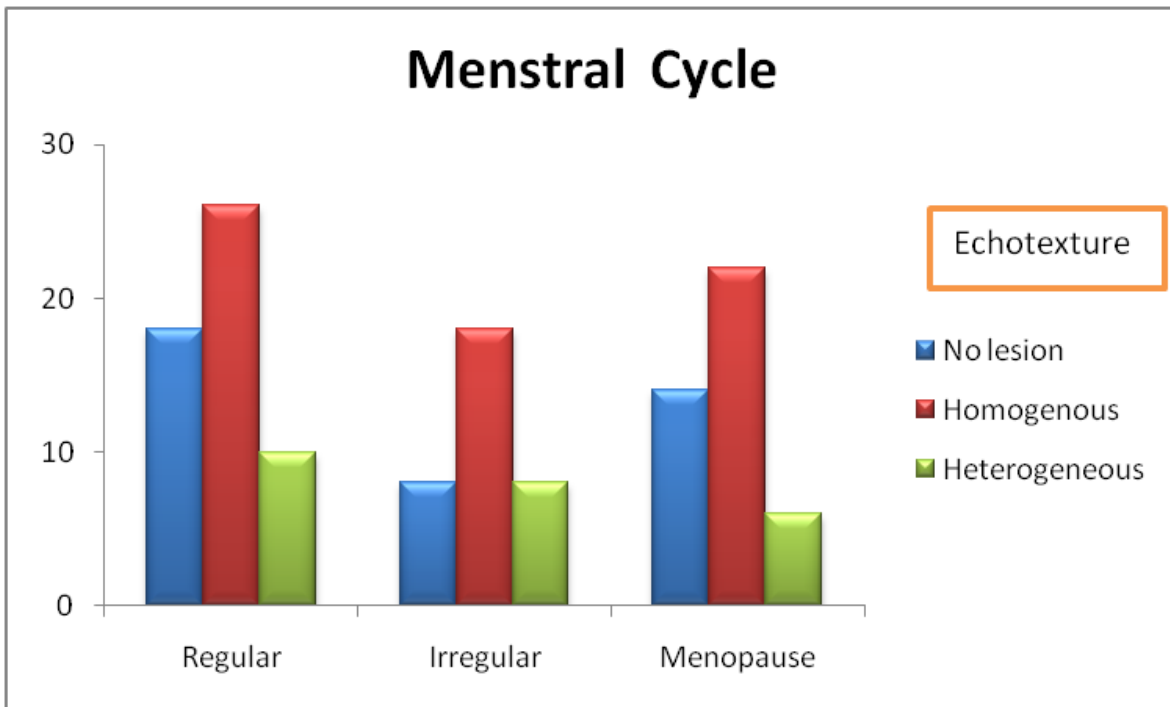
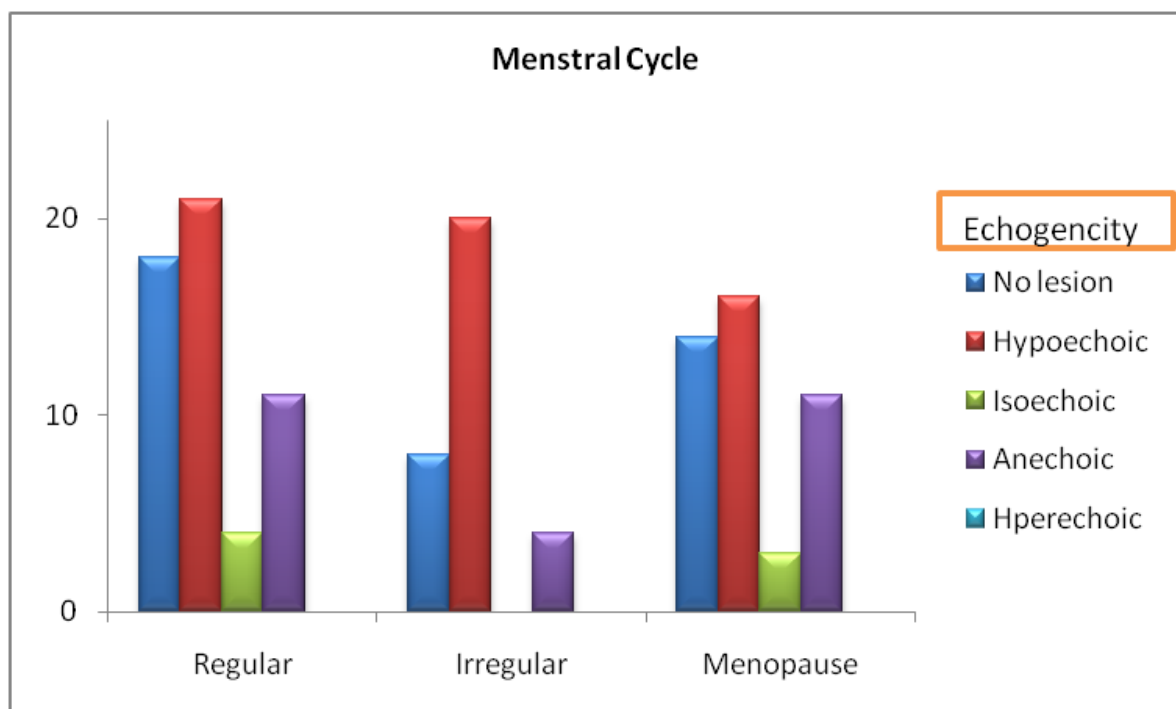


Figure (4.13). Cross tabulation showed the relation between the menstrual cycle lesion and echotexture

Table 4.9. Cross tabulation showed the relation between the menstrual cycle and lesions echogenicity

		Lesion Echogenicity					Total
		No lesion	Hypoechoic	Isoechoic	Anechoic	Hyperechoic	
menstrual cycle	Regular	18	21	4	11	0	54
	Irregular	8	20	0	4	0	32
	Menopause	14	16	3	11	0	44
Total		40	57	7	26	0	130
Correlation is significant at $P < 0.05$ , $p = 0.274$							



Figure(4.14) Bar graph showed the relation between menstrual cycle and lesion echogenicity

Table 4.10. Cross tabulation showed the relation between Breast feeding and lesions echogenicity

		Echogenicity					Total
		No lesion	Hypoechoic	Isoechoic	Anechoic	Hyperechoic	
Breast Feeding	Yes	24	34	7	18	0	83
	No	16	23	0	8	0	47
Total		40	57	7	26	0	130
Correlation is significant at $P < 0.05$ , $p = 0.274$							

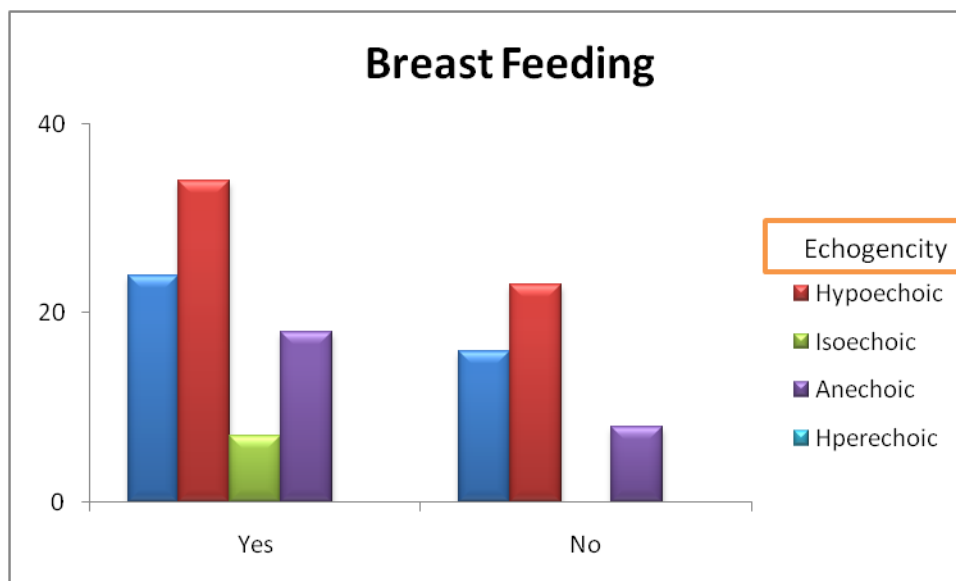


Figure (4.15). Bar graph showed the relation between the breast feeding and lesion echogenicity

Table 4.11. Showed the relation between the breast feeding and lesions morphology

		Morphology			Total
		No lesion	Solitary	Multiple	
Breast feeding	No	17	5	35	57
	Yes	23	10	40	73
Total		40	15	75	130
Correlation is significant at $P < 0.05$ , $p = 0.49$					

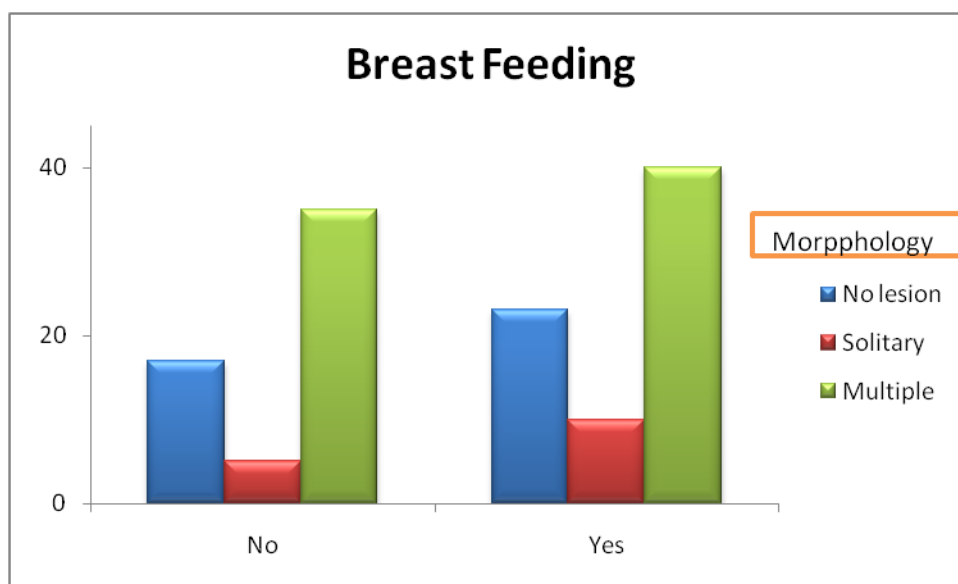


Figure (4.16). Showed the relation between the breast feeding and lesions morphology



Table 4.12 Showed tabulation of breast family history finding

		Breast Finding		Total
		Positive	Negative	
Family history	No	7	63	70
	Yes	5	56	60
Total		11	119	130
Correlation is significant at $P < 0.05$ , $p = 0.24$				

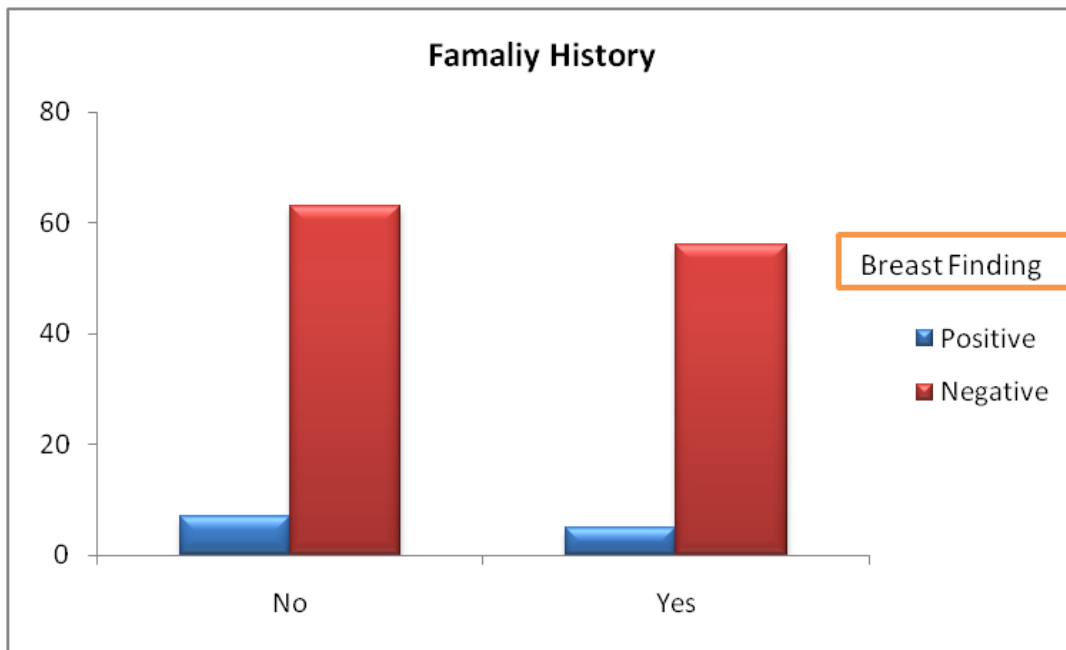


Figure (4.17). Cross tabulation Showed Family history of breast finding

Table 4.13 Showed vascularity frequency distribution percentage of breast lesions

	No lesion	A Vascular	Central Vascular	Prevascular	Total
Frequency	40	80	4	6	130
Percentage	30.7	61.5	3	4.6	100%

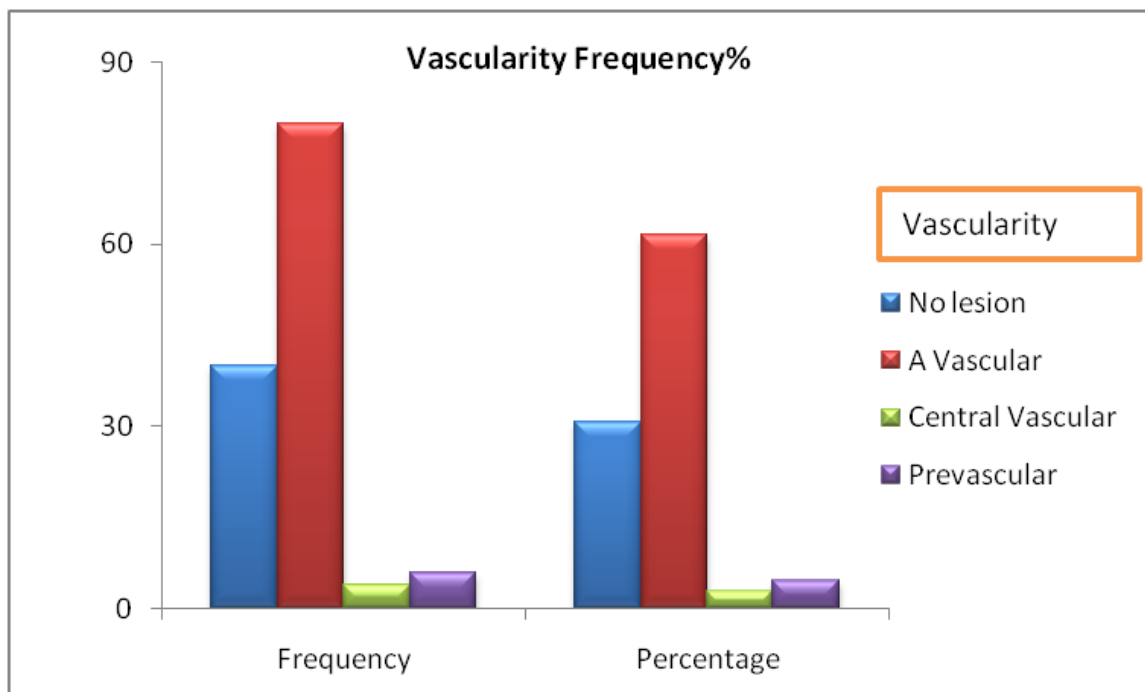


Figure (4.18). Showed vascularity frequency percentage of breast lesions.

## Chapter five

### Discussion, Conclusion and Recommendation

#### 5.1. Discussion:

Firstly the classification was aimed to extract these feature from the image based on the normal image histogram where the primary image (figure 4.1.) was converted into tiff format as an input image for IDL image processing program, then a window of 3x3 was created in order to scan the image then the feature were extracted for three different images of US containing three classes which are Fibroadenoma, breast cyst and relative to the normal fibroglandular tissue and the feature were include; mean; variance; coarseness; skewness; kurtosis; energy; and entropy. All these feature were calculated for all images and then the data were ready for discrimination which was performed using step-wise technique in order to select the most significant feature that can be used to classify the Fibroadenoma in US images which give best demonstration during the scan for three selected classes and the result showed that: Table (1). Linear discriminant function and the overall classification accuracy equal to 95% and 100%, 92.8% classification sensitivity for Fibroadenoma, cyst and fibroglandular tissue respectively with classification specificity of 92.5% were computed from gray level histogram and the results are represented that there is a well concentration of features around the class centers which give a remarkable difference among the three classes especially between the cyst and normal breast tissues in the mean of gray level feature as in Figure (4.3) however, No clear difference in the energy was seen between the cyst and fibroglandular tissue while both are clearly separated from the Fibroadenoma in which indicate that the Fibroadenoma can be differ from these classes because of different texture in US as in figure (4.5). Among all phases of ultrasound scan the

Fibroadenoma reveal different texture for entropy and mean while having low texture feature for energy feature.

Linear discriminate analysis was used to classify the Fibroadenoma, and breast tissue, so the features of the classified regions of the whole images (as raw data) were classified furthers. The result of the classification showed that the Fibroadenoma were classified well from the normal breast tissues even though it has characteristics similar to surrounding tissue, and the texture reveal a different underlying pattern compared to the breast and cyst with classification sensitivity 100%, and the combination of the texture features throughout the different US image phases provides the highest predictive overall accuracy of 95% using linear discriminant analysis. Images with the same slice location were analyzed simultaneously using both US and texture correlation. In this way the texture evolution during the propagation of the sound-wave was taken into account. The method was applied to recognizing normal breast and its two main pathology understudy. Experiments with various sets of texture parameters and two classification methods showed that a simultaneous analysis of texture parameters derived from three subsequent acquisition moments considerably improved the classification accuracy). Also the lesion was examined and the image was tested using 3x3 matrix size (window) based on the intensity profile of the scanned image and this performed in order to differentiate the pathology under study from the normal tissue because of similarity that may note in component of these classes. Finally, excellent discrimination between Fibroadenoma, cyst and normal fibroglandular tissue can be established on the basis as few as three optimal feature among the 18 texture characteristics tested. This serves as a second method to perform more characterization of such tumor.

This part of the study conclude that Fibroadenoma, cyst of the breast and other breast tissue in US images for simplicity can be diagnosed and classify by using the following simple equation after extracting the associated features using a window of 3×3 pixel from the region of interest; the biggest classification score assume the tissue type :

$$\text{Fibroadenoma} = (\text{mean} * 1.62) + (\text{energy} * 0.03) + (\text{entropy} * -0.175) - 26.834$$

$$\text{Breast cyst} = (\text{mean} * 1.02) + (\text{energy} * 0.064) + (\text{entropy} * -0.119) - 12.062$$

$$\text{Fibroglandular normal tissue} = (\text{mean} * 0.913) + (\text{energy} * 0.06) + (\text{entropy} * -0.065) - 45.086$$

This study also intended to characterize the lesion using ultrasound feature in case of Fibroadenoma and cystic lesion also many parameter related to the patient was selected to be correlated and identify if it has a significant effect on these conditions as follow: The role of sonography in breast imaging in primary and secondary breast cancer screening examination in patients who have dense breasts on mammography. In all four studies, sonography detected approximately three carcinomas that were missed by primary screening mammography per 1000 patients. The lesions were missed on mammography because they did not contain calcifications and were obscured by surrounding or superimposed dense tissues on the mammogram.

Also U/S characterization was one of the focus of this study in which all examination the images were extracted and then interpreted to final diagnosis in order to assess the Fibroadenoma relative to its US character so that the result showed, 41% with regular outline indicate the benignancy of disease, 30.7% with normal result and more than 95% with breast feeding, 46.5% form all women having hypoechoic lesion, with homogenous echotexture in 54.4% of the patient, no calcification seen, 61.5% A vascular and pre vascularity was noted in 4.6 % of lesion mostly near the vascularity of breast. UOQ commonly affected in both breast.

This study reveals that the minimum age at time of diagnosis can be close to the 16 year and the mean age equal to 41.8yrs in which the SD indicate the relatively greater variation in age of the patient, mass size is not significant variable here because the evaluation totally not depend on the mass size although it depend on the character of the mass and its related variables. As in table (4-2)

A strong relation noted between the maternal status and the lesion of the breast in with relatively equal percentage of can affect both breast RT and LT possibly due to the age related breast lesion obesity and hormonal stimulations, where the normal cases was 30 patient complaining of the symptoms but the result was negative for both breast. As in table 4- 3. Figure (4.7). Correlation is significant at  $P < 0.05$ ,  $p = 0.448$ .

As well majority of the affected patient was married and only two pregnancy showed strong relation between the texture and maternal status in which more than 60 patient having homogenous echotexture for while small frequency noted for heterogeneity of the disease, this mostly related to the composition of breast in which low density associated with age more than 30 for married people. Correlation is significant at  $P < 0.05$ ,  $p = 0.431$ , as in table 4. Figure (4.8)

Echogenicity of the lesion under study both Fibroadenoma and the breast cyst tend to have hypoechoic lesion rather than hyperechogenicity because these tissue is containing fluids in case of cyst and relatively hyperechogenicity in case of Fibroadenoma a strong correlation noted at  $p = 0.9$  as in table 5. Figure (2.10). Maternal status having a strong tendency of multiple lesion rather than solitary one as in table (6) figure (2-11) at  $p = 0.93$ . Homogenous echotexture was predominant in case of patient with regular, irregular or menopausal women correlation is significant at  $P < 0.05$ ,  $p = 0.564$ .

Figure (2.15). Cross tabulation showed the relation between the breast feeding and the echogenicity of the disease in which the majority of the patient having multiple lesion rather than one lesion or else so that indicate the breast feeding having strong relation with the morphology of the disease whether it benign or cystic changes. (Correlation is significant at  $P < 0.05$ ,  $p = 0.49$ ). As in table (4-10) figure (2.16).

Relatively significant association was noted between the family history and the breast feeding in which more than 90% of case having positive family history that agree with the disease of breast are common in older age rather than the younger one as in table (4-11). Figure (2.17).

Table (4-13) Figure (4.17). Cross tabulation showed vascularity frequency percentage of breast lesions about 61.5 % of all patients had no vascular , 3% with central vascular while 4.6% had pre vascularity.

## **5.2. Conclusion:**

This study was aimed to use texture analysis and classification methods to characterize the breast Fibroadenoma, cyst and normal breast regions in U/S images using image processing program (IDL). An analytical case control study of Breast US images of 130 adult subjects with Fibroadenoma, cyst and normal fibrogranular tissue images that in which used as entry data. U/S characterization was one of the focus of this study in which all examination the images were extracted and then interpreted to final diagnosis in order to assess the Fibroadenoma and cyst relative to US character. The study found that the Fibroadenoma texture reveal a different underlying pattern compared to the cyst and normal breast tissues with classification sensitivity and specificity 100% and 92.5% respectively for fibroadenoma, and the combination of the texture features throughout the different U/S image phases provide the highest predictive overall accuracy of 95% using linear discriminant analysis technique.

So ultrasound is of value examination to differentiate between breast fibroadenoma and cyst, Study showed that Doppler ultrasound is standard, from percentage of A vascular, prevascularity and central vascularity.

From texture analysis point of view it can be used to do new for breast anatomy.



### **5.3. Recommendation:**

- Texture analysis can be integrated in ultrasonography as Computer Aided Diagnosis method to reduce the operator dependent concept in ultrasound field and hence reduce using of unnecessary fine meddle aspiration.
- Young patient with positive family history must be followed and screened routinely by ultrasound and texture analysis to detect small dense lesion that can be missed by mammogram.
- Texture analysis tools are not usually available, and it is expensive. According to its high values in diagnosis of breast lesion and differentiation between it is types, study advised that to indorse it, until becomes available to any radiology department and patient.
- Further studies should be carried out in this field on many aspects such as increasing the number of patients, to show the relation between normal breast fibro glandular tissue fibro adenoma and cyst .
- Also Further studies should be carried, diagnosis of breast morphological result and consideration of scanning time to be equal in all patients.
- Compare between the role of U/S scanning and other diagnostic tools using color Doppler .
- To add biopsy result to computer .

## References:

El-Wakeel H, Umpleby HC. Systematic review of fibroadenoma as a risk factor for breast cancer. *Breast* 2003;12:302–307.

Hughes LE, Mansel RE, Webster DJT. Aberrations of normal development and involution (ANDI): a new perspective on pathogenesis and nomenclature of benign breast disorders. *Lancet* 1987;2:1316–1319.

Tavassoli FA, ed. Chapter 11. Biphasic tumors. In: *Pathology of the Breast, Second Edition*. Stamford, CT: Appleton & Lange, 1999:571–631.

Kleer CG, Tseng MD, Gutsch DE et al. Detection of Epstein-Barr virus in rapidly growing fibroadenomas of the breast in immunosuppressed hosts. *ModPathol* 2002;15:759–764.

Moore T, Lee AHS. Expression of CD34 and bcl-2 in phyllodes tumours, fibroadenomas and spindle cell lesions of the breast. *Histopathology* 2001;38:62–67.

Donegan WL. Common benign conditions of the breast. In: Donegan WL, Spratt JS, eds. *Cancer of the Breast, Fifth Edition*. St. Louis, MO: Saunders, 2002:67–110.

K.KirkShung. *Medical imaging physics 4th Ed*. Raton London NEW YORK (NY): CRC press; 2002.P. 308-310.

Hendee,WR.*Medical imaging physics 4th Ed*. New York (NY): Willey less;. 2002.P.10

Drake, Richard L.; Vogl, Wayne; Tibbitts, Adam W.M. Mitchell; illustrations by Richard; Richardson, Paul (2005). *Gray's anatomy for students*. Philadelphia: Elsevier/Churchill Livingstone.

Stöppler, Melissa Conrad. "Breast Anatomy". Retrieved 28 June 2015.

Doucet, Sébastien; Soussignan, Robert; Sagot, Paul; Schaal, Benoist (2009).

Hausberger, Martine, ed. "The Secretion of Areolar (Montgomery's) Glands from Lactating Women Elicits Selective, Unconditional Responses in Neonates". *PLoS ONE* 4 (10): e7579. doi:10.1371/journal.pone.0007579. PMC 2761488.PMID 19851461.

Pamplona DC, de Abreu Alvim C. Breast Reconstruction with Expanders and Implants: a Numerical Analysis. *Artificial Organs* 8 (2004), pp. 353–356.

Wood K, Cameron M, Fitzgerald K (2008). "Breast Size, Bra Fit and Thoracic Pain in Young Women: A Correlational Study". *Chiropractic & Osteopathy* 16:1.doi:10.1186/1746-1340-16-1. PMC 2275741. PMID 18339205.

Lauersen, Niels H.; Stukane, Eileen (1998). *The Complete Book of Breast Care* (1st Trade Paperback ed.). New York: Fawcett Columbine/Ballantine.

Rinker, B; Veneracion, M; Walsh, C (2008). "The Effect of Breastfeeding on Breast Aesthetics". *Aesthetic Surgery Journal* 28 (5): 534–7.doi:10.1016/j.asj.2008.07.004. PMID 19083576. Lay summary – LiveScience(November 2, 2007).

Araco, A.; Gravante, G.; Araco, F.; Gentile, P.; Castrì, F.; Delogu, D.; Filingeri, V.; Cervelli, V. (22 May 2006). "Breast Asymmetries: A Brief Review and Our Experience". *Aesthetic Plastic Surgery* 30 (3): 309–319. doi:10.1007/s00266-005-0178-x. Retrieved 27 June 2015.

Diane Scutt; Gillian A Lancaster; John T Manning. "Breast Asymmetry and Predisposition to Breast Cancer". MedScape. Retrieved 28 June 2015.

Piccoli, Catherine W.; Feig, Stephen A.; Palazzo, Juan P. (April 1999). "Developing Asymmetric Breast Tissue<sup>1</sup>". *Radiology* 211 (1): 111–117.doi:10.1148/radiology.211.1.r99ap42111.

Robert L. Barbieri (2009), "Yen & Jaffe's Reproductive Endocrinology"(PDF), Yen (6th ed.) (Elsevier): 235–248, doi:10.1016/B978-1-4160-4907-4.00010-3

Maxwell GP, Gabriel A. Breast Reconstruction. In: Aston SJ, Steinbrech DS, Walden JL. Aesthetic Plastic Surgery. Philadelphia, Pa: Elsevier; 2009:chap 57.

Jones, GE, ed. Bostwick's Plastic and Reconstructive Breast Surgery. 3rd ed. St. Louis, Mo: Quality Medical Pub; 2010.

Mathes SJ, Nahai F. Reconstructive Surgery: Principles, Anatomy, and Technique. New York, NY: Churchill Livingstone; 1997.

Rees TD, LaTrenta GS. Aesthetic Plastic Surgery. 2nd ed. Philadelphia, Pa: WB Saunders; 1994.

Thorne CH, Beasley RW. Grabb and Smith's Plastic Surgery. 6th ed. Philadelphia, Pa: Wolters Kluwer Health/Lippincott Williams and Wilkins; 2007

Lauersen, Niels H.; Stukane, Eileen (1998). The Complete Book of Breast Care (1st Trade Paperback ed.). New York: Fawcett Columbine/Ballantine.

Rinker, B; Veneracion, M; Walsh, C (2008). "The Effect of Breastfeeding on Breast Aesthetics". Aesthetic Surgery Journal 28 (5): 534–7.doi:10.1016/j.asj.2008.07.004. PMID 19083576. Lay summary – LiveScience(November 2, 2007).

Bentley, Gillian R. (2001). "The Evolution of the Human Breast". American Journal of Physical Anthropology 32 (38): 30–50. doi:10.1002/ajpa.1033.

Ricardo L. Rodriguez, MD ,"Breast Lift Procedure".. Retrieved 29 January2012.

Younai, S. Sean. "Breast Sagging – Ptosis". Retrieved 26 January 2012.

Rinker B, Veneracion M, Walsh CP (2010). "Breast ptosis: causes and cure". Ann PlastSurg 64 (5): 579–84. doi:10.1097/SAP.0b013e3181c39377.PMID 20354434.

Campolongo, Marianne (5 December 2007). "What Causes Sagging Breasts?". Retrieved 26 January 2012.

Caleffi M, Filho DD, Borghetti K et al. Cryoablation of benign breast tumors: evolution of technique and technology. *Breast* 2004;13:397–407.

Kelsey JL, Gammon MD. Epidemiology of breast cancer. *Epidemiol Rev* 1990;12:228–240

La Vecchia C, Parazzini F, Franceschi S et al. Risk factors for benign breast disease and their relation with breast cancer risk. Pooled information from epidemiologic studies. *Tumori* 1985;71:167–178.

Donegan WL. Common benign conditions of the breast. In: Donegan WL, Spratt JS, eds. *Cancer of the Breast, Fifth Edition*. St. Louis, MO: Saunders, 2002:67–110.

Pfeifer JD, Barr RJ, Wick MR. Ectopic breast tissue and breast-like sweat gland metaplasias: an overlapping spectrum of lesions. *J Cutan Pathol* 1999;26:190–196.

Marshall MB, Moynihan JJ, Frost A et al. Ectopic breast cancer: case report and literature review. *Surg Oncol* 1994;3:295–304.

Tewari M, Shukla HS. Breast tuberculosis: diagnosis, clinical features & management. *Indian J Med Res* 2005;122:103–110.

van Diest PJ, Beekman WH, Hage JJ. Pathology of silicone leakage from breast implants. *J Clin Pathol* 1998;51:493–497.

Passaro ME, Broughan TA, Sebek BA et al. Lactiferous fistula. *J Am Coll Surg* 1994;178:29–32.

Rosen PP, ed. Chapter 4. Specific infections. In: *Rosen's Breast Pathology, Second Edition*. Philadelphia: Lippincott Williams & Wilkins, 2001: 65–75.

Furlong AJ, al-Nakib L, Knox WF et al. Periductal inflammation and cigarette smoke. *J Am CollSurg* 1994;179:417–420.

Rahal RMS, de Freitas-Junior R, Paulinelli RR. Risk factors for duct ectasia. *Breast J* 2005;11:262–265.

Dixon JM, Ravisekar O, Chetty U et al. Periductal mastitis and duct ectasia: different conditions with different etiologies. *BrJSurg* 1996;83:820–822.

Rosai J, ed. Chapter 20. Breast. In: Rosai and Ackerman's Surgical Pathology, Ninth Edition. Philadelphia: Mosby, 2004:1763–1876.

Kinoshita T, Yashiro N, Yoshigi J et al. Fat necrosis of breast: a potential pitfall in breast MRI. *Clin Imaging* 2002;26:250–253.

Silverberg SG, Masood S. The breast. In: Silverberg SG, DeLellis RA, Frable WJ, eds. Principles and Practice of Surgical Pathology and Cytopathology, Third Edition. New York: Churchill-Livingstone, Inc., 1997:575–673.

Love SM, Gelman RS, Silen W. Fibrocystic “disease” of the breast--a non-disease? *N Engl J Med* 1982;307:1010–1014.

Santen RJ, Mansel R. Benign breast disorders. *N Engl J Med* 2005;353:275–285.

Vorherr H. Fibrocystic breast disease: pathophysiology, pathomorphology, clinical picture, and management. *Am J Obstet Gynecol* 1986;154:161–179.

O'Malley FP, Bane AL. The spectrum of apocrine lesions of the breast. *AdvAnatPathol* 2004;11:1–9.

Houssami N, Irwig L, Ung O. Review of complex breast cysts: implications for cancer detection and clinical practice. *ANZJ Surg* 2005;75:1080–1085.

Venta LA, Kim JP, Pelloski CE et al. Management of complex breast cysts. *AJR Am J Roentgenol* 1999;173:1331–1336.

Vargas HI, Vargas MP, Gonzalez KD et al. Outcomes of sonography-based management of breast cysts. *Am J Surg* 2004;188:443–447.

Lee K, Chan JKC, Gwi E. Tubular adenosis of the breast: a distinctive benign lesion mimicking invasive carcinoma. *Am J Surg Pathol* 1996;20:46–54.

Jensen RA, Page DL, Dupont WD et al. Invasive breast cancer risk in women with sclerosing adenosis. *Cancer* 1989;64:1977–1983.

Gill HK, Ioffe OB, Berg WA. When is a diagnosis of sclerosing adenosis acceptable at core biopsy? *Radiology* 2003;228:50–57.

Millis RR, Eusebi V. Microglandular adenosis of the breast. *Adv Anat Pathol* 1995;2:10–18.

Eusebi V, Foschini MP, Betts CM et al. Microglandular adenosis, apocrine adenosis, and tubular carcinoma of the breast: an immunohistochemical comparison. *Am J Surg Pathol* 1993;17:99–109.

Acs G, Simpson JF, Bleiweiss IJ et al. Microglandular adenosis with transition into adenoid cystic carcinoma of the breast. *Am J Surg Pathol* 2003;27:1052–1060.

Tavassoli FA, ed. Chapter 5. Benign lesions. In: *Pathology of the Breast, Second Edition*. Stamford, CT: Appleton & Lange, 1999:115–204.

Vina M, Wells CA. Clear cell metaplasia of the breast: a lesion showing eccrine differentiation. *Histopathology* 1989;15:85–92.

Tavassoli FA, ed. Chapter 6. Ductal intraepithelial neoplasia. In: Pathology of the Breast, Second Edition. CT: Appleton & Lange, 1999:205–323.

Koerner FC. Epithelial proliferations of ductal type. *SeminDiagn Pathol* 2004;21:10–17.

Page DL, Dupont WD, Rogers LW et al. Atypical hyperplastic lesions of the female breast. A long-term follow-up study. *Cancer* 1985;55:2698–2708.

Dupont WD, Page DL. Relative risk of breast cancer varies with time since diagnosis of atypical hyperplasia. *Hum Pathol* 1989;20:723–725.

Page DL, Schuyler PA, Dupont WD et al. Atypical lobular hyperplasia as a unilateral predictor of breast cancer risk: a retrospective cohort study. *Lancet* 2003;361:125–129.

Schnitt SJ, Vincent-Salomon A. Columnar cell lesions of the breast. *AdvAnatPathol* 2003;10:113–124.

Schnitt SJ. The diagnosis and management of pre-invasive breast disease: flat epithelial atypia – classification, pathologic features and clinical significance. *Breast Cancer Res* 2003;5:263–268.

Kennedy M, Masterson AV, Kerin M et al. Pathology and clinical relevance of radial scars: a review. *J ClinPathol* 2003;56:721–724.

Patterson JA, Scott M, Anderson N et al. Radial scar, complex sclerosing lesion and risk of breast cancer. Analysis of 175 cases in Northern Ireland. *Eur J SurgOncol* 2004;30:1065–1068.

Rabban JT, Sgroi DC. Sclerosing lesions of the breast. *SeminDiagnPathol* 2004;21:42–47.

Oyama T, Koerner FC. Noninvasive papillary proliferations. *SeminDiagnPathol* 2004;21:32–41.



MacGrogan G, Tavassoli FA. Central atypical papillomas of the breast: a clinicopathological study of 119 cases. *Virchows Arch* 2003;443:609–617.

Pacilli M, Sebire NJ, Thambapillai E et al. Juvenile papillomatosis of the breast in a male infant with Noonan syndrome, café au lait spots, and family history of breast carcinoma. *Pediatr Blood Cancer* 2005;45:991–993.

Haj M, Weiss M, Herskovits T. Diabetic sclerosing lymphocytic lobulitis of the breast. *J Diabetes Complications* 2004;18:187–191.

Baratelli GM, Riva C. Diabetic fibrous mastopathy: sonographic-pathologic correlation. *J Clin Ultrasound* 2005;33:34

Castro CY, Whitman GJ, Sahin AA. Pseudoangiomatous stromal hyperplasia of the breast. *Am J ClinOncol* 2002;25:213–216.

Pruthi S, Reynolds C, Johnson RE et al. Tamoxifen in the management of pseudoangiomatous stromal hyperplasia. *Breast J* 2001;7:434–439.

Mercado CL, Naidrich SA, Hamele-Bena D et al. Pseudoangiomatous stromal hyperplasia of the breast: sonographic features with histopathologic correlation. *Breast J* 2004;10:427–432.

Franco N, Arnould L, Mege F et al. Comparative analysis of molecular alterations in fibroadenomas associated or not with breast cancer. *Arch Surg* 2003;138:291–295.

Valdes EK, Boolbol SK, Cohen JM et al. Malignant transformation of a breast fibroadenoma to cystosarcomaphyllodes: case report and review of the literature. *Am Surg* 2005;71:348–353.

Geisler DP, Boyle MJ, Malnar KF et al. Phyllodes tumors of the breast: a review of 32 cases. *Am Surg* 2000;66:360–366.

Chen WH, Cheng SP, Tzen CY et al. Surgical treatment of phyllodes tumors of the breast: retrospective review of 172 cases. *J Surg Oncol* 2005;91:185–194.

Carter BA, Page DL, Schuyler P et al. No elevation in long-term breast carcinoma risk for women with fibroadenomas that contain atypical hyperplasia. *Cancer* 2001;92:30–36.

Shabtai M, Saavedra-Malinger P, Shabtai EL et al. Fibroadenoma of the breast: analysis of associated pathological entities--a different risk marker in different age groups for concurrent breast cancer. *Isr Med Assoc J* 2001;3:813–817.

Graf O, Helbich TH, Fuchsjaeger MH et al. Follow-up of palpable circumscribed noncalcified solid breast masses at mammography and US: can biopsy be averted? *Radiology* 2004;233:850–856.

Wechselberger G, Schoeller T, Piza-Katzer H. Juvenile fibroadenoma of the breast. *Surgery* 2002;132:106–107.

Lanng C, Eriksen BO, Hoffmann J. Lipoma of the breast: a diagnostic dilemma. *Breast* 2004;13:408–411.

Reeves ME, Tabuenca A. Lactating adenoma presenting as a giant breast mass. *Surgery* 2000;127:586–588.

Baker TP, Lenert JT, Parker J et al. Lactating adenoma: a diagnosis of exclusion. *Breast J* 2001;7:354–357.

Montemarano AD, Sau P, James WD. Superficial papillary adenomatosis of the nipple: a case report and review of the literature. *J Am AcadDermatol* 1995;33:871–875.

Gatti G, Mazzarol G, Simsek S et al. Breast hamartoma: a case report. *Breast Cancer Res Treat* 2005;89:145–147.

Herbert M, Sandbank J, Liokumovich P et al. Breast hamartomas: clinicopathological and immunohistochemical studies of 24 cases. *Histopathology* 2002;41:30–34.

Tse GMK, Law BKB, Ma TKF et al. Hamartoma of the breast: a clinicopathological review. *J ClinPathol* 2002;55:951–954.

Montagnese MD, Roshong-Denk S, Zaher A et al. Granular cell tumor of the breast. *Am Surg* 2004;70:52–54.

Ilvan S, Ustundag N, Calay Z et al. Benign granular-cell tumour of the breast. *Can J Surg* 2005;48:155–156.

Balzan SMP, Farina PS, Maffazzioli L et al. Granular cell breast tumour: diagnosis and outcome. *Eur J Surg* 2001;167:860–862.

Howlett DC, Marchbank NDP, Allan SM. Sonographic assessment of symptomatic breast – a pictorial review. *J Diagnostic Radiography & Imaging*. 2003;5:3–12.

Stavros AT. The Breast. In: Rumack CM, Wilson SR, Charboneau JW, editors. *Diagnostic Ultrasound*. 3rd ed. St Louis: M, Elsevier Mosby; 2005. p. 828.

Shetty MK, Shah Y. Sonographic Findings in Focal Fibrocystic Changes of the Breast. *Ultrasound Quarterly*. 2002;18:35–40.

Stavros AT. Benign Solid Nodules: Specific pathologic diagnosis. In: Stavros AT, editor. *Breast Ultrasound*. Vol. 13. Lippincot Williams & Wilkins; 2004. pp. 528–96.

Maniero MB, Goldkamp A, Lazarus E, Livingston L, Koelicker SL, Schepps B, Mayo-Smith WW. Characterization of Breast Masses with Sonography. *J Ultrasound Med*. 2005;24:161–7.

Meyberg-Solomayer GC, Kraemer B, Bergmann A, Kraemer E, Krainick U, Wallwiener D, Solomayer EF. Does 3-D sonography bring any advantage to noninvasive breast diagnostics? *Ultrasound Med Biol.*2004;30:583–9.

R. M Haralick., K. Shanmugam& I. Dinstein. 1973. Textural feature for image classification. *IEEE Trans. Man, Cybern*, 6:610-621.

Bassett LW, Kimme-Smith C. Breast sonography. *American Journal of Roentgenology*, 1991; 156:449-455

Egan RL. *Breast Imaging: Diagnosis and Morphology of Breast Diseases*. Philadelphia, WB Saunders, 1988, pp. 100-125

Fornage BD. *Ultrasound Of The Breast*. In: *Ultrasound Quarterly*, Vol. 11, No. 1: 1-39, Raven Press Ltd., New York, 1993.

Kopans DB, Meyer TE, Sadowsky N. Breast imaging. *The New England Journal of Medicine*, 1984; 310:960-967

Wilson ARM, Teh WL. *Ultrasound Of The Breast*. *Imaging* 9: 169-185, 1997. (1997 *Science and Technology Letters*

## Appendix (A) Ultrasound Images

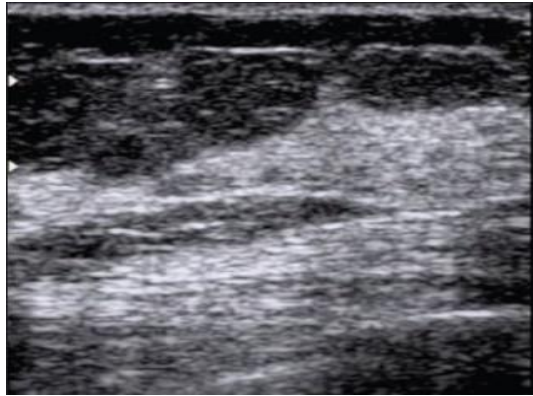


Figure :( 5 -1) Show mid transverse scan of a normal breast, fibroglandular parenchyma is echogenic and is surrounded by hypoechoic fat , female

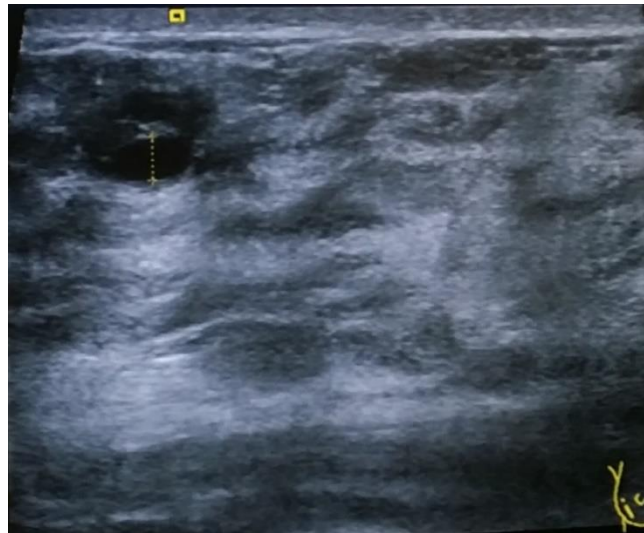


Figure (5A-2) Show RLOQ breast cysts in 28 years old female measure 4x3mm



Figure (5A-3) show RLOQ breast cysts in 54 years old female

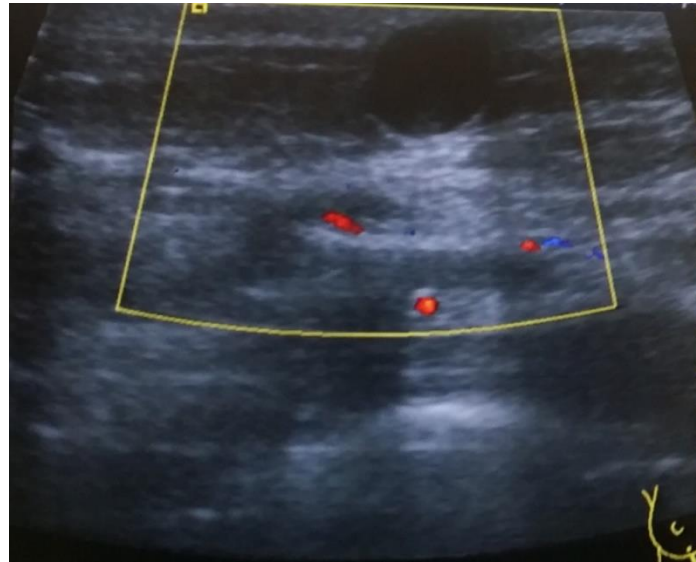


Image (A- 4) show Rt. breast large retareola cyst 3x2.5cm in female 49 years old

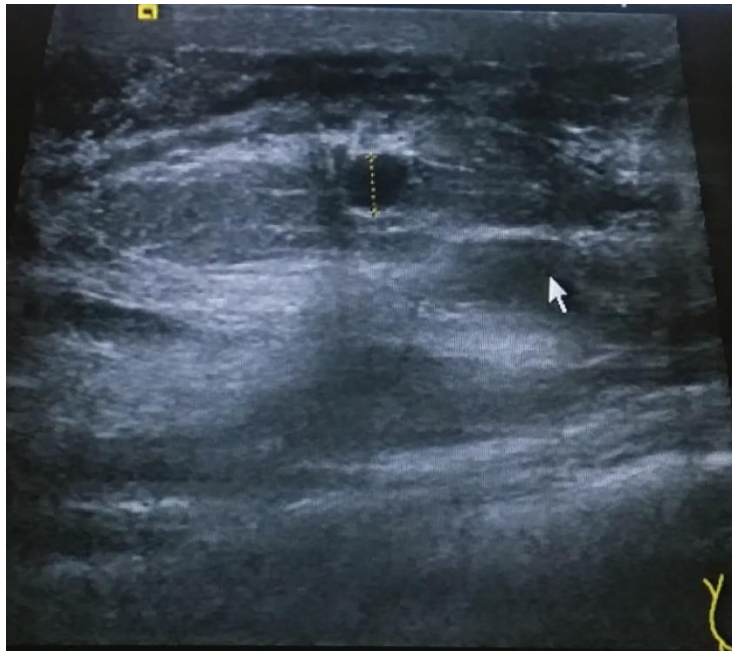


Figure (5A-5) Show RUOQ breast small cysts in 42years old female

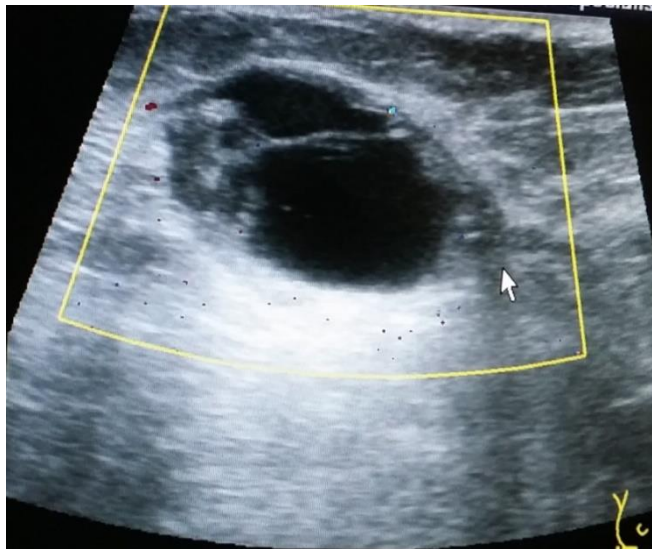


Figure (A-6) 68years old female with Rt. Breast RLOQ cyst measure 3x2cm

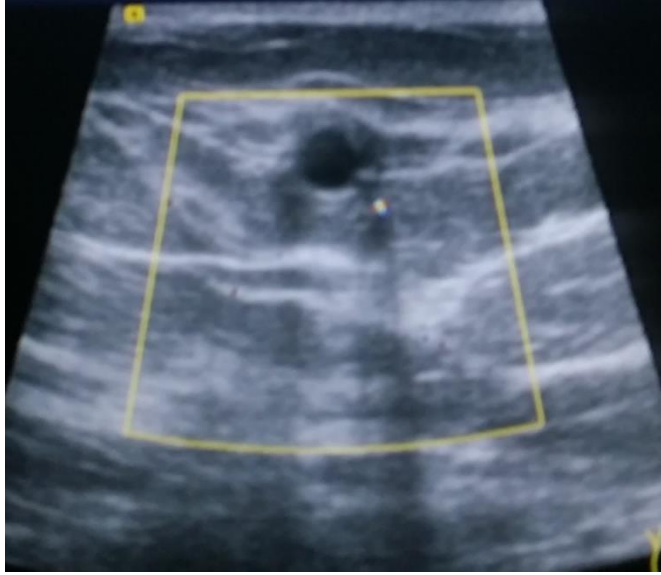


Figure (5A-7) 40 years old female with Rt. Breast RLOQ cyst



Figure (5A-8) show LUOQ breast small cysts in 32years old female



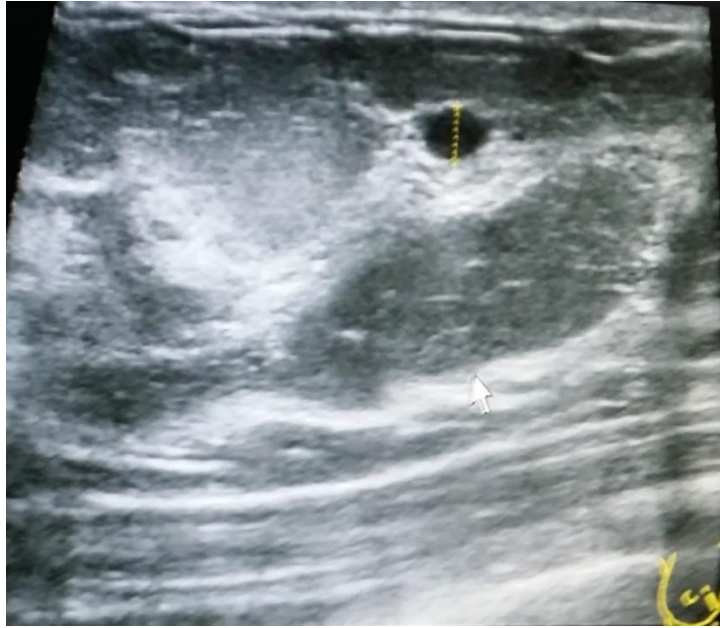


Image (5A- 9) Show Rt. Breast small cyst at UOQ in 47 years old female measure 5x5mm

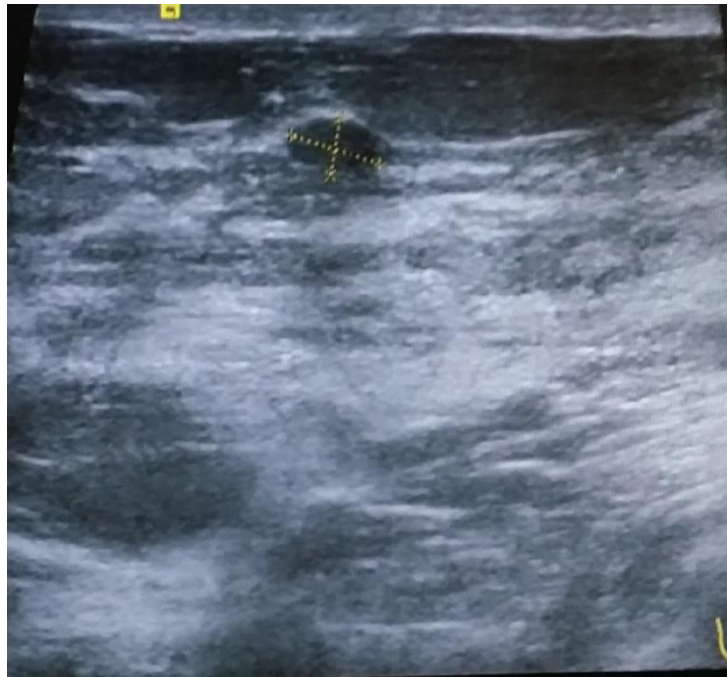


Figure (5A-10) Show well defined hypoechoic LUOQ breast +Fibroadenoma measuring 8x4 in 48 years old female

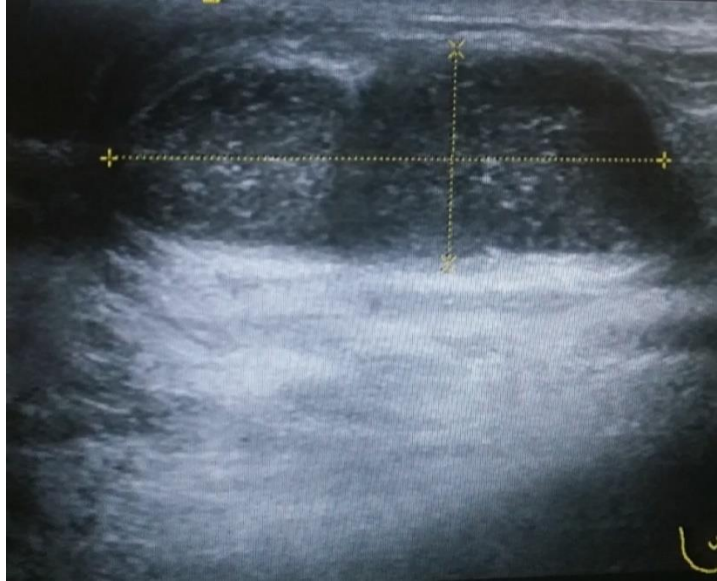


Figure (5A-11) Show well defined oval macro lobulated hypoechoic in LUOQ breast Fibroadenoma measuring 3x1 cm , 16years old female

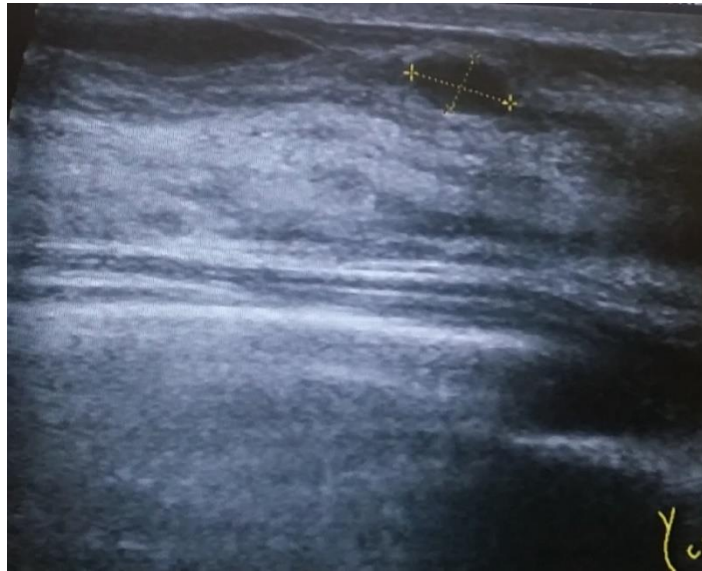


Figure (5A-12) Show well defined oval hypoechoic in LUOQ breast Fibroadenoma measuring 8x5 mm , 29 years old female

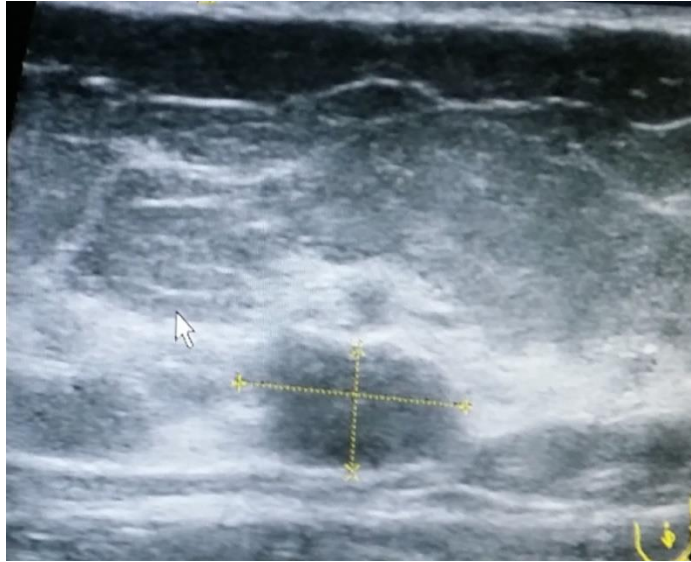


Figure (5A-13) Show stable well defined hypoechoic LUOQ breast Fibroadenoma measuring 13x7 , in 68 years old female

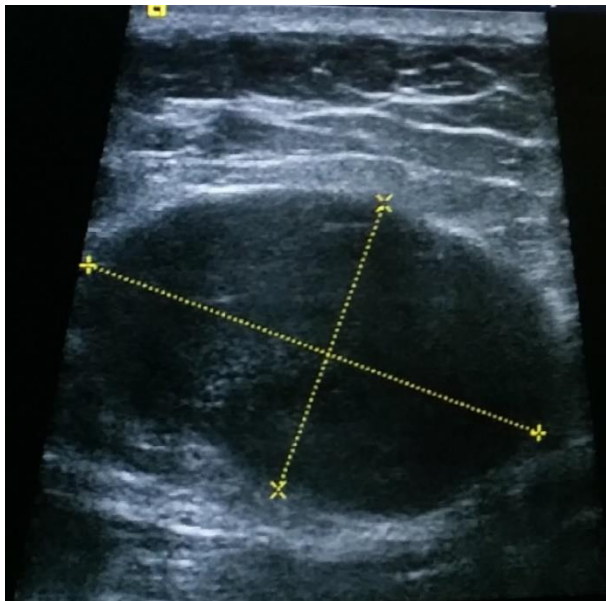


Figure (5A-14) show well defined oval macro lobulated hypoechoic in LLOQ breast Fibroadenoma measuring 44 x 26 cm , 32 years old female

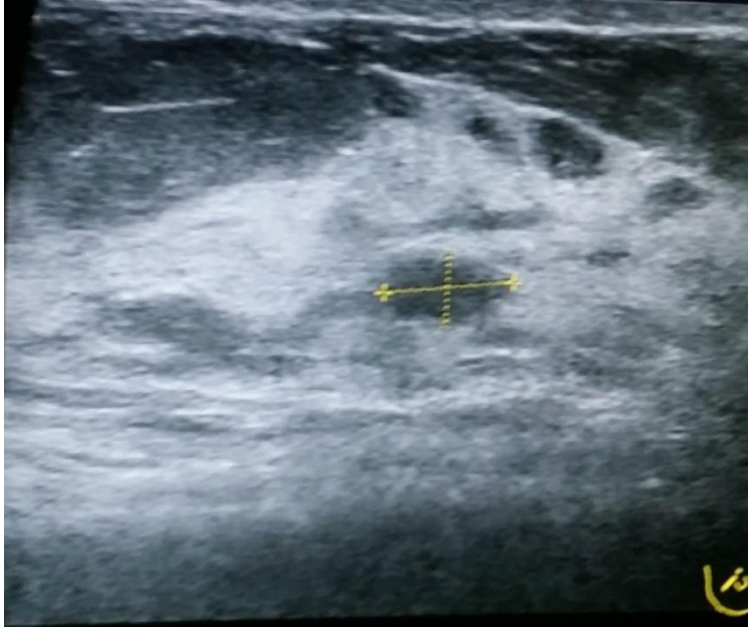


Figure (5A-15) Show well defined hypoechoic LUOQ breast +Fibroadenoma measuring 10x5,  
56 years old female

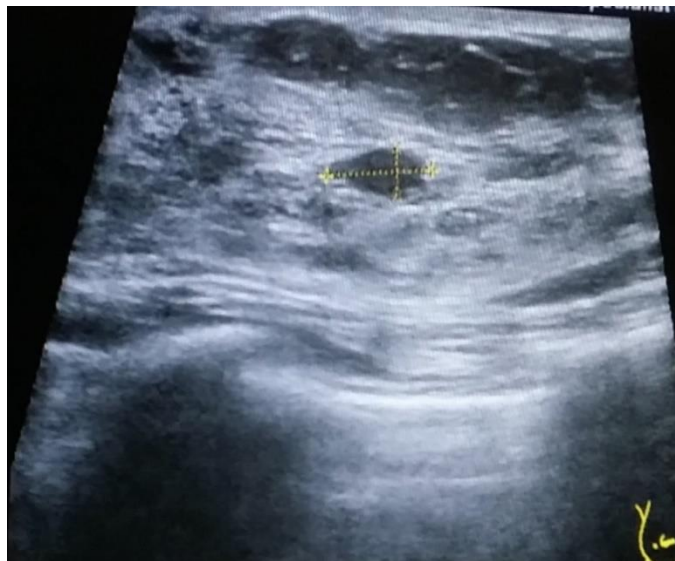


Figure (5A-16) Show well defined hypoechoic RUOQ breast Fibroadenoma measuring 7x4, in  
40 years old female

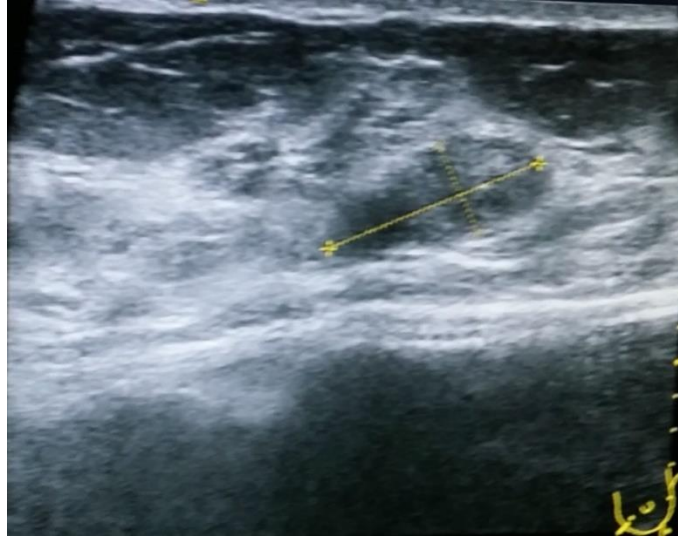


Figure (5A- 17) Show well defined hypoechoic LUOQ breast Fibroadenoma measuring 12x16, in 30 years old female

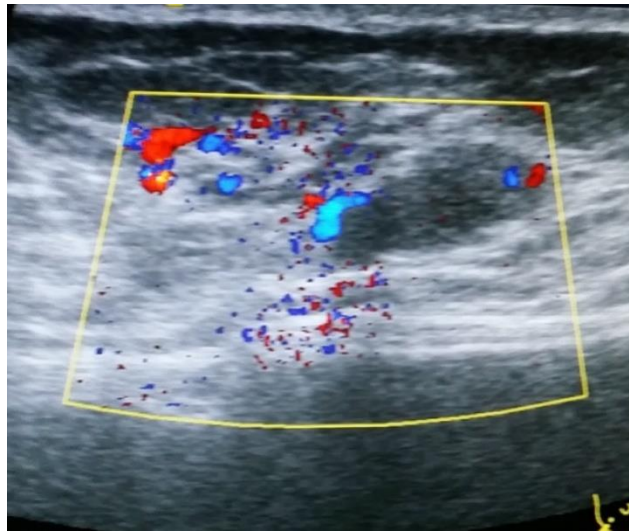


Figure (5A- 18) Show oval well defined hypoechoic LUOQ breast Fibroadenoma measuring 12x26 , in 36 years old female





Figure (5A-19) Show well defined hypoechoic LUOQ breast Fibroadenoma,48 years old female  
measure 7x4 mm

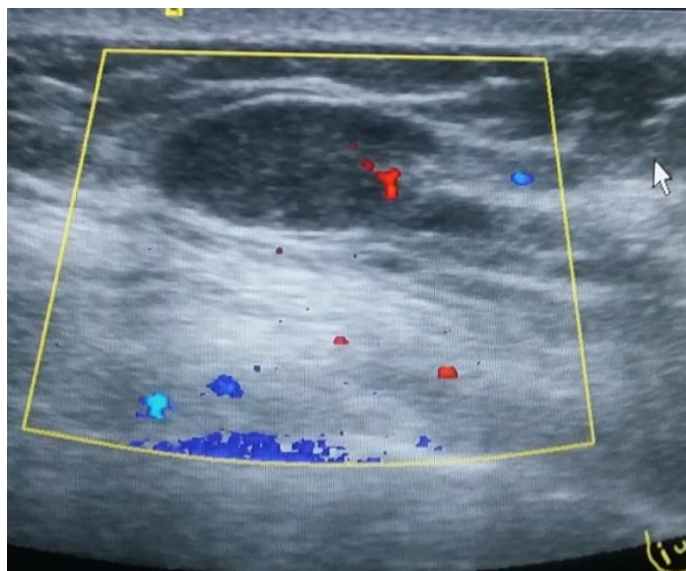


Figure (5A-34) Show oval well defined hypoechoic LUOQ breast Fibroadenoma measuring  
9x24, in 29 years old female

## Appendix (B)

### Data collection

Age	Maternal status	Pour	Breast feeding	Menstrual cycle	Breast finding	Sit e	Move ment	Mass size	Weigh t	Heigh t	Mass contor	Echogenci ty
40	1	1	1	1	1	1	1	1050	93	153	1	2
37	1	0	0	1	1	1	2	33	75	150	1	4
46	1	0	0	0	1	1	2	435	89	165	2	2
46	1	5	1	2	1	2	1	109	60	150	1	2
50	1	3	1	3	1	1	2	60	65	160	1	4
55	1	8	1	3	1	1	1	72	95	170	1	2
51	1	6	1	3	1	1	1	72	83	167	1	3
25	1	2	0	1	0	0	0	0	95	153	0	0
41	1	3	1	2	1	2	1	45	80	160	1	2
26	1	0	0	1	1	1	1	12	58	155	2	2
28	0	0	0	2	0	0	0	0	54	150	0	0
33	1	1	1	2	1	1	2	30	84	156	1	4
32	1	2	1	1	1	1	1	8	68	166	1	2
65	1	0	0	3	1	2	2	726	66	156	2	0
65	1	4	0	3	0	0	0	0	66	165	0	0
53	1	5	1	3	1	1	1	54	63	160	1	4
59	1	5	1	3	1	2	2	2080 0	65	159	2	0
47	1	4	1	3	0	0	0	0	64	160	0	0
19	1	9	1	3	1	1	2	88	60	162	1	2
33	1	3	0	1	1	0	0	0	100	170	0	0
80	1	6	1	3	1	1	2	425	78	150	1	4
47	1	0	0	1	1	0	0	0	108	158	0	0
50	1	5	1	3	1	1	2	33	75	160	1	2
47	1	6	1	3	1	0	0	0	70	157	0	4
31	1	2	0	1	1	1	2	280	58	152	1	4
31	1	3	1	1	1	1	1	9	103	160	1	2
30	1	4	1	1	1	1	1	72	57	153	1	4

64	1	5	1	3	1	0	0	0	60	162	1	2
16	0	0	0	1	1	2	1	2640	43	158	1	2
47	1	4	1	1	1	1	2	17	90	162	1	3
52	1	0	0	3	1	1	2	20	80	158	1	2
68	1	6	1	3	1	2	1	16	60	150	1	2
40	1	4	1	1	1	0	0	0	86	162	0	0
29	1	4	1	2	1	1	1	45	65	152	1	2
33	1	0	1	1	1	1	1	24	74	155	1	4
45	1	1	0	2	1	2	1	0	81	146	1	2
49	1	3	1	2	1	1	2	403	94	145	1	2
34	1	4	1	1	1	0	0	0	65	152	0	0
69	1	0	0	3	1	2	1	120	105	165	1	4
22	0	0	0	1	1	1	2	8	58	158	1	4
26	1	4	1	1	1	1	1	12	70	152	1	4
42	1	5	1	1	1	0	0	0	74	152	0	0
28	1	1	1	1	1	0	0	0	74	155	0	0
51	1	2	0	3	1	0	0	0	86	160	0	0
66	1	2	1	3	1	2	2	8	72	155	1	2
52	1	5	1	3	1	0	0	0	84	160	0	0
53	1	3	0	3	1	0	0	0	80	166	0	0
39	1	8	1	3	1	2	0	0	74	154	0	0
29	1	1	1	1	1	2	1	20	60	160	1	2
43	1	2	0	2	1	2	2	20	58	152	1	2
29	1	2	1	1	1	0	0	0	68	155	0	0
28	1	1	0	1	1	2	2	12	49	156	1	2
26	1	1	1	1	1	0	0	0	68	162	0	0
53	1	3	1	3	1	2	1	25	69	164	1	2
59	1	8	0	3	1	1	0	0	82	150	1	4
38	1	1	0	2	1	1	2	8	47	158	1	0
57	1	6	1	3	1	0	0	12	64	164	1	4
71	1	3	1	3	1	1	2	1612 8	82	145	2	2
30	1	2	0	1	1	1	1	0	83	164	2	2



35	1	5	1	2	1	0	0	0	64	124	0	0
46	1	6	1	2	1	2	2	60	104	158	1	4
43	1	2	1	2	1	1	1	120	54	155	1	2
43	1	2	0	1	1	0	0	0	81	110	0	0
58	1	8	0	3	1	1	1	159	75	160	1	2
28	0	0	0	2	1	1	1	120	76	153	1	2
35	1	3	0	1	1	1	1	72	67	168	1	2
29	1	2	0	2	1	2	1	1197	94	150	1	2
17	0	0	0	1	1	0	0	0	47	153	0	0
56	1	6	0	3	1	1	1	157	79	160	1	2
28	0	0	0	2	1	2	2	0	75	155	1	2
24	0	0	0	1	1	1	2	3120 0	59	159	1	2
56	1	6	0	3	1	1	2	5940	74	160	0	0
48	1	6	0	2	1	1	2	19	69	160	1	2
45	1	1	0	2	1	2	2	39	63	153	1	2
51	1	4	0	3	1	0	0	0	75	155	0	0
43	1	3	0	2	1	1	2	60	89	160	1	2
46	1	5	1	2	1	1	2	166	82	155	1	2
45	1	3	1	1	1	1	1	12	75	160	1	2
53	1	5	1	3	1	0	0	0	85	156	0	0
49	1	0	0	1	1	1	2	72	94	158	1	4
42	1	0	0	2	1	0	0	0	70	152	0	0
48	1	4	1	1	1	1	0	8	90	165	0	2
39	1	4	1	1	1	1	2	57	65	152	1	2
52	1	5	1	3	1	1	2	111	79	159	1	2
36	1	4	1	1	1	1	0	0	65	150	0	0
40	1	1	1	1	1	2	1	55	93	153	1	2
50	1	3	1	3	1	2	2	8640	65	160	1	2
55	1	8	1	3	1	2	1	108	95	170	1	2
51	1	6	1	3	1	2	1	30	83	167	1	3
26	1	0	0	1	1	2	1	12	58	155	2	0
32	1	2	1	1	1	2	1	12	68	166	1	2

3	1	5	1	3	1	2	1	46	63	160	1	4
47	1	4	1	1	1	2	2	116	90	162	1	3
50	1	0	0	3	1	2	2	8	80	158	1	2
68	1	6	1	3	1	1	1	273	60	150	1	2

## **Appendix (C) Published Papers**

### **Paper 1**

International Journal of Science and Research (IJSR) ISSN (Online): 2319-7064 Index  
Copernicus Value (2015): 78.96 | Impact Factor (2015): 6.391 Volume 6 Issue 3, March 2017  
www.ijsr.net Licensed Under Creative Commons Attribution CC BY

### **Frequency Distributions of Feature Used to Characterize Breast Fibroadenoma in U/S**

**Amal mammon<sup>1</sup>, Mohammed Elfadil<sup>2</sup>, A. H. A. Bakry<sup>3 1, 2, 3</sup>**

Sudan University of Science and Technology, College of Medical Radiologic Science,  
Crossing Elguish St. and Elshahid Elzabier St. Former Elbaldia Street, Khartoum, Sudan

### **Paper 2**

### **Characterization of Breast Fibroadenoma in U/S Images Using Image Texture Analysis Techniques**

**Amal mammon<sup>1</sup>, Mohammed Elfadil<sup>1</sup>, A. H. A. Bakry<sup>1</sup>**

<sup>1</sup>Sudan University of Science and Technology, College of Medical Radiologic Science,  
Crossing Elguish St. and Elshahid Elzabier St. Former Elbaldia Street, Khartoum, Sudan